JOURNAL OF FOOD PROCESS ENGINEERING

JOURNAL OF FOOD PROCESS ENGINEERING

JOURNAL OF FOOD PROCESS ENGINEERING

Journal of
FOOD PROCESS ENGINEERING

VOLUME 7
NUMBER 4

Editor: D. R. HELDMAN

CONTENTS

MEETINGS

March, 1985

3/5–3/7 Food Pack '85. Gainesville Hilton, Gainesville, Florida. Contact H. M. Beckman, The Packaging Institute, USA, 20 East 46th Street, New York, New York 10017.

3/4–3/8 International Symposium on Food Irradiation Processing. Co-sponsored by FAO and International Atomic Energy Agency. Washington, D.C. Contact Hans-Friedrich Meyer, Director of Public Information IAEA, Wagramerstrasse 5, P.O. Box 100, A1400, Vienna, Austria.

3/11–3/13 Better Process Control School. University of Washington, Seattle Washington, Seattle Washington. Contact J. Matches, Institute of Food Science & Technology, University of Washington, Seattle, Washington 98195.

3/12–3/13 Fiber in Food Conference. John M. Clayton Hall Conference Center, University of Delaware, Newark, Delaware. Contact S. Brocka, University of Delaware, John M. Clayton Hall, Newark, Delaware 19711.

3/18–3/21 Better Process Control School. University of Minnesota, St. Paul, Minnesota. Contact Dr. E. A. Zottola, Dept. of Food Science & Nutrition, University of Minnesota, St. Paul, Minnesota 55108.

3/19–3/22 39TH Annual Meeting of the R&D Associates. San Antonio, Texas. Contact Colonel Merton Singer, Executive Director, R&D Associates, 103 Biltmore Drive, Suite 106, San Antonio, Texas 78213.

3/25–3/29 Better Process Control School. The Ohio State University, Columbus, OH. Contact W. A. Gould, Dept. of Horticulture, Ohio State University, 2001 Fyffe Court, Columbus, OH 43210.

3/25–3/26 International Symposium on Pasta & Extruded Cooked Foods. Sponsored by Institute of Pharmacology and Pharmacognosy of the University of Milan, Milan, Italy. Contact Dr. I. Ceserani, Pasta and Extruded Cooked Foods, Tecnoalimenti, Via Balcaaretti 9, 20133 Milan, Italy.

3/26–3/29 Better Process Control School. University of Maryland, Virginia Polytechnic Institute and Rutgers University, Easton, Maryland. Contact R. C. Willey, University of Maryland, Dept. of Horticulture, College Park, Maryland 20742.

3/24–3/28 Spring National Meeting of the American Institute of Chemical Engineers. Astro Hall, Houston, TX. Contact Beth Van Dijk. AIChE, 345 East 47th Street, New York, N. Y. 10017.

April,1985

4/1–4/4 Better Process Control School, University of Wisconsin, Madison, Wisconsin. Contact C. E. Johnson Dept. of Food Science, Babcock Hall, Madison, Wisconsin 53706.

4/8–4/11 Better Process Control School. University of California, Davis, California. Con-

tact R. C. Pearl, Dept. of Food Science & Technology, University of California, Davis, California 95616.

4/10–4/12 International Symposium on Chemistry & Physics of Baking: Materials, Processes & Products. Contact T. Gailliard, RHM Research Limited, the Lord Rank Research Center, Lincoln Road High Wycombe, Bucks HB12 3QR, U.K.

4/15–4/18 Better Process Control School. Purdue University, W. Lafayette, Indiana. Contact J. V. Chambers, Dept. of Food Science, Smith Hall, Purdue University, W. Lafayette, Indiana 47907.

4/29–5/2 Better Process Control School. Pennsylvania State University, University Park Pennsylvania. Contact G. D. Kuhn, Dept. of Food Science, 16 Borland Building, Pennsylvania State University, University Park, Pennsylvania 16802.

May, 1985

5/6–5/9 Better Process Control School. Cornell University, Rochester, N.Y. Contact D. L. Downing, Cornell University, Dept. of Food Science & Technology, Geneva, N.Y. 14456.

5/7 - 5/9 10th Powder & Bulk Solids Conference. O'Hare Exhibition Center, Rosemont, Illinois. Contact Cahners Exhibition Group, Cahners Plaza, 1350 Touhy Avenue, Dex Plains, Illinois 60018.

5/19 - 5/24 Fourth Joint Convention & Workshop of the Australian Institute of Food Science & Technology and the New Zealand Institute of Food Science and Technology. University of Cantebury, Christ Church, New Zealand. Contact the Convention Secretariat, Foodanza 85, Guthreysnz Tours Limited P.O. Box 343, Christ Church, New Zealand.

June, 1985

6/9 - 6/12 45TH Annual Meeting and Food Expo of the Institute of Food Technologists. Georgia World Congress Center, Atlanta, GA. Contact C. L. Willey, Institute of Food Technologists, Suite 2120, 221 N. LaSalle Street Chicago, IL 60601.

6/23 - 6/26 Summer Meeting of the American Society of Agricultural Engineers. Michigan State University, East Lansing, Michigan. Contact M. A. Purschwitz, American Society of Agricultural Engineers, 2950 Niles Road, P.O. Box 410, St. Joseph, Michigan 49085.

6/23 - 6/26 The 28th Annual Conference of the Canadian Institute of Food Science and Technology. Royal York Hotel, Toronto, Canada. Contact T. Koorneef Marketing & Publicity Food Pro National Inc., 1589 the Queen's Way, #2 Toronto, Ontario M8Z5W9, Canada.

July, 1985

7/7 - 7/10 Fourth International Congress on Engineering and Food. Edmonton, Alberta, Canada. Contact M. LeMaguer, Dept. of Food Science, 2-06 AgFor Center, University of Alberta, Edmonton, Alberta, Canada T6G2P5.

7/14 - 7/17 Second International Conference on Fouling and Cleaning in Food Processing. Madison, Wisconsin. Contact Daryl Lund, Dept. of Food Science, 1605 Linden Drive, Madison, Wisconsin 53706.

7/22 - 7/26 Fourth Controlled Atmosphere Research Conference, Raleigh, N.C. Contact W. E. Bellinger, Dept. of Horticultural Science, North Carolina State University, Box 5216, Raleigh, N.C. 27650.

7/23 - 7/26 Fourth International Flavor Conference on the Shelf Life of Foods and Beverages. Rhodes, Greece. Contact C. J. Mussinan, International Flavors & Fragrances, 1515 State Highway 36, Union Beach, N.J. 07735

August, 1985

8/5 - 8/9 72nd Annual Meeting of the International Association of Milk Food & Environmental Sanitarians. Hyatt Regency-Nashville, Tenn. Contact K. R. Hathaway IAMFES, Inc.—P.O. Box 701, Ames, Iowa 50010.

8/25 - 8/28 1985 Summer National Meeting of the American Institute of Chemical Engineers. Western Hotel-Seattle, Washington. Contact Beth Van Dijk, AIChE, 345 E. 47th Street, New York, N.Y. 10017.

THROUGHPUT AND POWER CONSUMPTION
OF DOUGH SHEETING ROLLS

LEON LEVINE

The Pillsbury Company
311 Second Street S.E.
Minneapolis, Minnesota 55414

ABSTRACT

Power law models of dough sheeting are shown to be inadequate in predicting sheeting roll energy input to doughs. Empirical modification of the theoretical model yields a model which predicts energy input to a dough for different roll sizes. The model indicates that energy input will be different for different size rolls. It is suggested that this is a source of difficulty when scaling up from laboratory to plant.

INTRODUCTION

The sheeting of doughs is quite common in the food industry. In the past, this was the method of choice for forming pasta products from semolina doughs. This process is described in detail by Hummel (1950). The use of sheeting for the production of sweet goods, biscuits, crackers and cookies is described by Matz (1968). A patent describing the use of sheeting for the production of fabricated potato chips is described by Curry (1976). There is a suggestion by Kilborn and Tipples (1974) that sheeting is an effective method for bread dough development.

There is some literature concerning the quantitative and qualitative effects of sheeting on dough quality. It has been shown (Feillet *et al.* 1975) that sheeting of pasta doughs causes a rearrangement of the protein network. These rearrangements increased with a reduction in roll clearance or an increase in the number of passages through the rolls. The effect of this rearrangement on finished noodle quality has been reported by Watanabe and Nagasawa (1968). This work reported increased rates of rehydration when the dough was subjected to increased sheetings.

Studies of the use of sheeting rolls for bread production emphasize the strong influence the rolls have on bread quality. Stenvert *et al.* (1979) suggests that the squeezing action of the rolls produces a very fine grained bread. They emphasize that because

of the energy imparted to the dough by the rollers, very stable doughs must be used. Moss (1980) reaches similar conclusions about the work done by the rolls. He suggests very stiff dough must be used to produce satisfactory bread by sheeting. Kilborn and Tipples (1974) are the only authors who report power consumption of the rolls. They find that dough development with sheeting rolls is very efficient, requiring only 10-15% of the energy normally required in the development of doughs via the more customary method of mixing. The experience of this author suggests that small changes in sheeting conditions will have significant effects on the properties of pastry doughs.

All of the above information suggests that a designer of sheeting lines must carefully consider power consumption when scaling-up the lines from a laboratory or pilot plant facility. There is no data available to perform this task.

Laboratory or pilot plant sheeting is typically done on small sets of rollers using multiple passes of the dough through successively smaller gaps. To simplify this procedure reversible rollers (fig. 1) are often used so that the dough passes through the rollers first in one direction and then the other, as roll spacing is reduced. This method is commonly used in small bakeries. These rollers are not exposed to much, stress, so only small diameter (3-4″) rolls are required. In a large capacity production facility, larger rollers are used, which are typically 6-12″ in diameter. In this case reduction is carried out by a series of rollers which gradually reduce the slab of dough to a continuous thin sheet of any desired dimension. The reduction in thickness in any roll might be as high as a factor of six, but a factor of two is more commonly used. Clearly a significant number of rolls may be required, and the path chosen to reduce the dough to its final thickness can greatly affect results. A set of 5-12″ rolls for reducing dough from approximately 2 in. to ¼ in. is illustrated in Fig. 2.

FIG. 1.   A REVERSIBLE SHEETER.
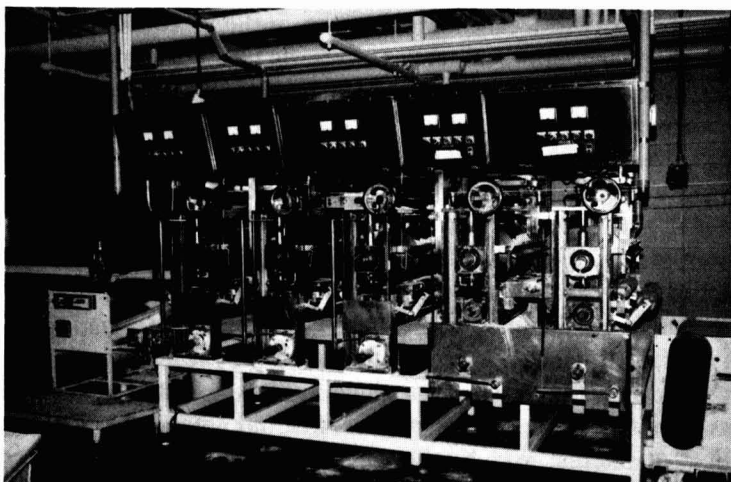
FIG. 2.   A FIVE-ROLL SHEETER.

It is the objective of this paper to illustrate the effect of sheeting roll size on energy input to the dough and to discuss the implications of roll scale-up.

MATERIALS AND METHODS

In this work, a "sweet dough" was studied. Viscosity was measured using a Haake Model #RV12 Rheometer, fitted with a #RVII cone and plate. A high tension spring was used to keep the cone and plate from separating. The viscometer was accelerated from 0 to 5 rpm over a five-minute period and direction of rotation was reversed.

Dough was reduced on 3.75 in. and 12 in. diameter rolls. The roll speeds studied ranged from 1-40 rpm on the 12 in. rolls, and from 125 to 200 rpm on the 3.75 in. rolls. Feed sheet thickness varied from 0.08 to 3 in. Roll gap was varied from 0.020 to 0.75 in.

THEORETICAL CONSIDERATIONS

Before discussing sheeting theory, a model of dough viscosity must be available. Dough is a complicated material which exhibits both viscous and elastic behavior. Many authors have reported the properties of dough measured by a variety of methods. Halton and Blair (1937) report values for apparent viscosity and shear modulus. Similar data is reported by Muller et al. (1961) and Schofield and Scott Blair (1932). These viscoelastic models are difficult to determine and very difficult to deal with mathematically.

A simpler approach is to treat the dough as a pseudoplastic fluid characterized by the power law model. There are several reports of the adequacy of this model. In mixing doughs, Hlynka (1962), reports a relationship between mixer speed and torque which suggests a power law fluid having a flow index of 0.5. Levine (1983) shows that for flow in extruders and dies, a hard wheat flour behaved like a power law fluid having a flow index of 0.41. Harper (1981) gives a power law equation for hard wheat flour undergoing shear between two cylinders, with a flow index of 0.35. Launay and Buré (1973), using a cone and plate viscometer, report values of the flow index in the range of 0.3 to 0.5.

The analogy between dough sheeting and calendering of plastics is useful in developing a model. Brazinsky et al. (1970) solved the problem of flow of a power law fluid between rollers. Their work is reviewed and extended by Middleman (1977). The equations for viscoelastic fluids are presented, but not solved by Chong (1968). An other article of interest may be the work of Elizarov et al. (1951).

A schematic description of the rolls is presented in Fig. 3. The output of this system, using the assumption applied by all previous authors is (Eq. 1):

$$Q = \pi D N t_o W \tag{1}$$

The outlet thickness of the sheet, t_o, is a dependent variable, which (according the literature) is a function of roll spacing, feed thickness, and a weak function of the flow index. For our area of interest, the graphical results of Brazinsky et al. (1970) may be approximated as (Eq. 2):

$$t_o \simeq 1.05 \, t_g \tag{2}$$

Equations 1 and 2 may be combined and rearranged into a dimensionless for to yield (Eq. 3):

$$\frac{Q}{ND^2W} \simeq 3.3 \left(\frac{t_g}{D} \right) \tag{3}$$

Because of the elastic nature of the dough, Eq. 3 is not an adequate predictor of final dough thickness. We have observed that the relaxed measurable dough thickness is a minimum of 15% greater than the roll spacing, but is usually much greater. The relaxed, final thickness is obviously an important product of the design of the rolls. Prediction of this value will be considered later in this paper.

Power consumption of the rolls is not given explicitly in the literature. A relationship may be developed by a simple extension. Following Middleman (1977), we can write (Eq. 4):

$$T_{xy} = \int_{y=0}^{y=h(x)} \left(\frac{dp}{dx} \right) dy \tag{4}$$
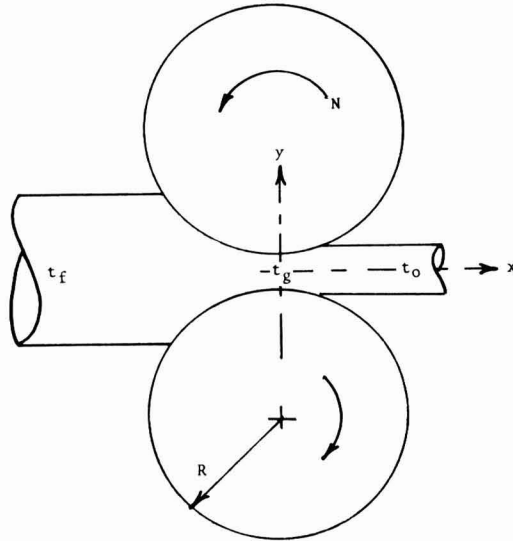
FIG. 3. SCHEMATIC REPRESENTATION OF ROLLS.

$$\text{where,} \quad T_{xy} = 0 \ @ \ y=0 \tag{4a}$$

$$\text{and,} \quad h(x) = H_g \left(1 + \frac{x^2}{2H_gR} \right) \tag{4b}$$

The power consumption is given by (Eq. 5):

$$P = 2WU \int_{\text{feed}}^{\text{discharge}} T_{xy}|_{y=h(x)} dx \tag{5}$$

where (Eq. 6),

$$T_{xy}|_{y=h(x)} = \left(\frac{dp}{dx} \right) H_g \left(1 + \frac{x^2}{2H_gR} \right) \tag{6}$$

The pressure gradient is defined by (Eq. 7):

$$\frac{dp}{dx} = - \left(\frac{2n+1}{n} \right) \frac{m}{\sqrt{2RH_g} \ (H_g/U)^n} \sqrt{\frac{2R}{H_g}} \frac{(\lambda^2 - \bar{x}^2)|\lambda^2 - \bar{x}|^{n-1}}{(1+\tilde{x}^2)^{2n+1}} \tag{7}$$

where:
$$\tilde{x} = \frac{x}{2RH_g} \tag{7a}$$

$$\lambda^2 = \frac{H_o}{H_g} - 1 \tag{7b}$$

After performing the indicated substitutions, and rearranging, Eq. 6 may be written as (Eq. 8):

$$N_{P_o} = \frac{1}{N_{R_e}} \left(\frac{H_g}{R}\right)^{\!1/2} G\left(n, \frac{H_f}{H_g}\right) \tag{8}$$

where, N_{P_o} is a power number, given by,

$$N_{P_o} = \frac{P}{\varrho N^3 R^4 W} \tag{8a}$$

N_{R_e} is Reynolds's number, given by,

$$N_{R_e} = \varrho N^{2-n} R^{2-n} H_g^n / m \tag{8b}$$

and,

$$G(n, H_f/H_g) = 2.82 \ (2\pi)^{1+n} \left(\frac{2n+1}{n}\right)^{\!n} \int_{feed}^{discharge} \frac{(\lambda^2 - \tilde{x}^2)|\lambda^2 - \tilde{x}|^{n-1} \ d\tilde{x}}{(1+\tilde{x}^2)^{2n}} \tag{8c}$$

The limits of integration are (Eq. 9):

feed:
$$\tilde{x} = -\left(\frac{H_f}{H_g} - 1\right)^{\!1/2} \tag{9}$$

discharge:
$$\tilde{x} = 0.224 \tag{9a}$$

For the discharge distance, we have assumed that Eq. 3 is a reasonable approximation. This greatly reduces the quantity of numerical evaluation required. Figure 4 is a plot of Eq. 8c for a flow index of 0.5.

EXPERIMENTAL RESULTS AND DISCUSSION

The viscosity obtained with the Haake Viscometer is illustrated in Fig. 5. For shear rates above 15 s^{-1}, several shear rates were chosen and the shear stress
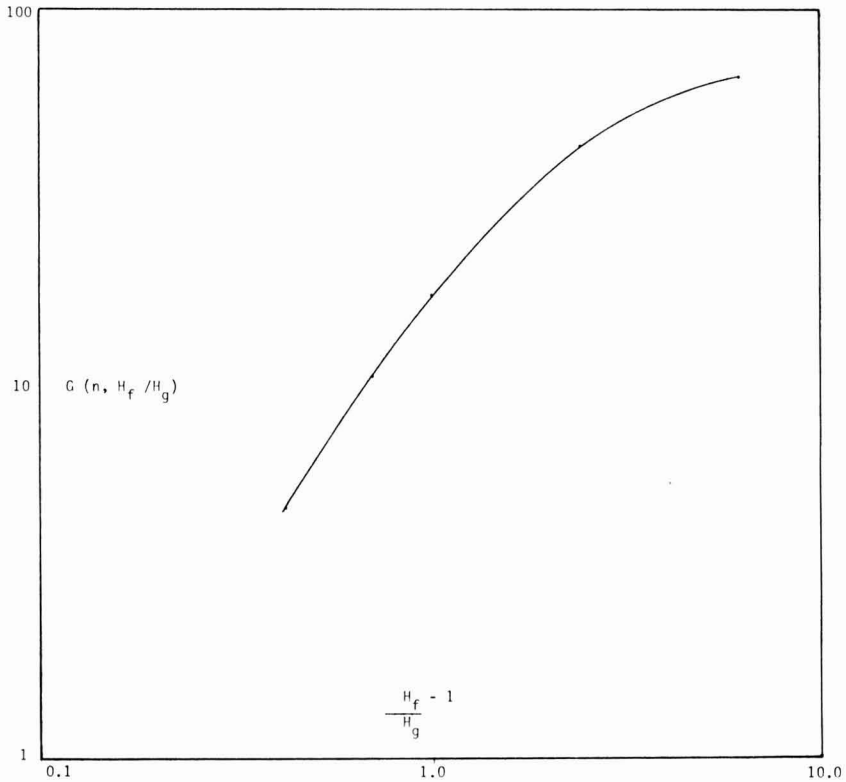
FIG. 4.   PLOT OF EQ. 8c FOR n=0.5.

recorded was averaged for the accelerating and decelerating parts of the curve. This data is plotted on Fig. 6. The data may be fitted to a power law model to obtain a viscosity model.

$$T = 1670 \; \dot{\gamma}^{\,0.5} \tag{10}$$

The data is described by a power law model very well, yielding a correlation coefficient (r^2) of 0.99. The flow index is within the range of previously reported values.

On Fig. 6, we have plotted data according to Eq. 4 for two different diameter rolls. We can see that Eq. 4 is an excellent approximation for actual performance of both sized rolls.

On Fig. 8, we have plotted power data for the 12 in. and 3.75 in. rolls in the form suggested by Eq. 8. There is significant scatter in the data, but we can see that Eq. 8 does not describe the performance of the rolls. The deviation is probably due to the inadequacy of the power law model.
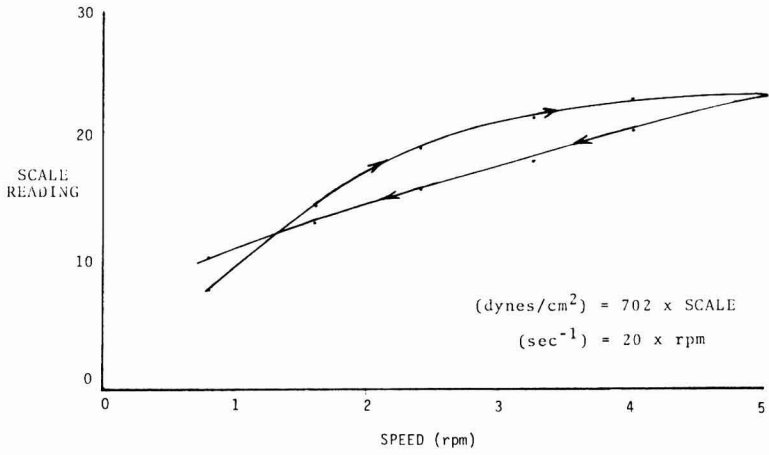
FIG. 5.   VISCOMETER OUTPUT VERSUS SPEED.
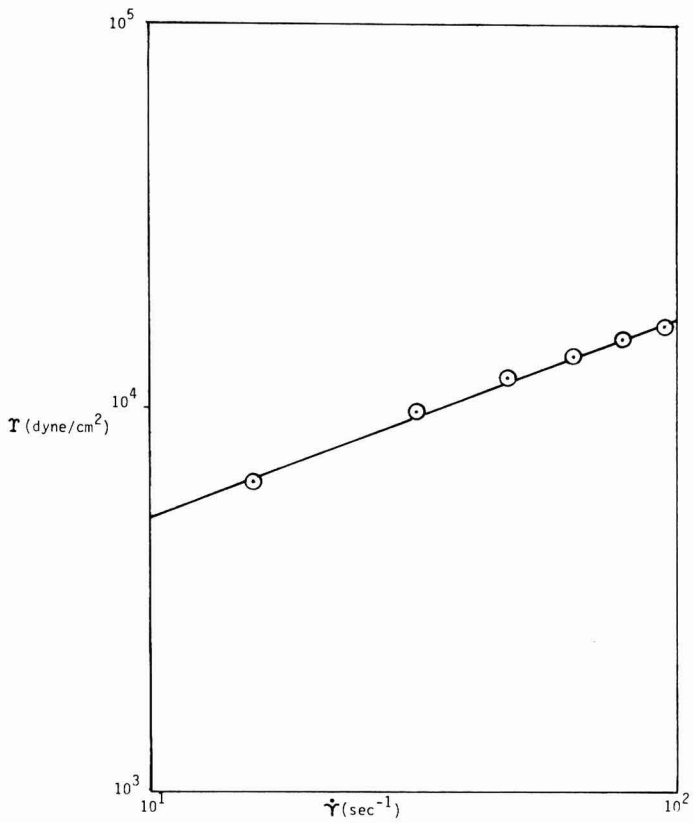
FIG. 6.   SHEAR STRESS VERSUS SHEAR RATE.
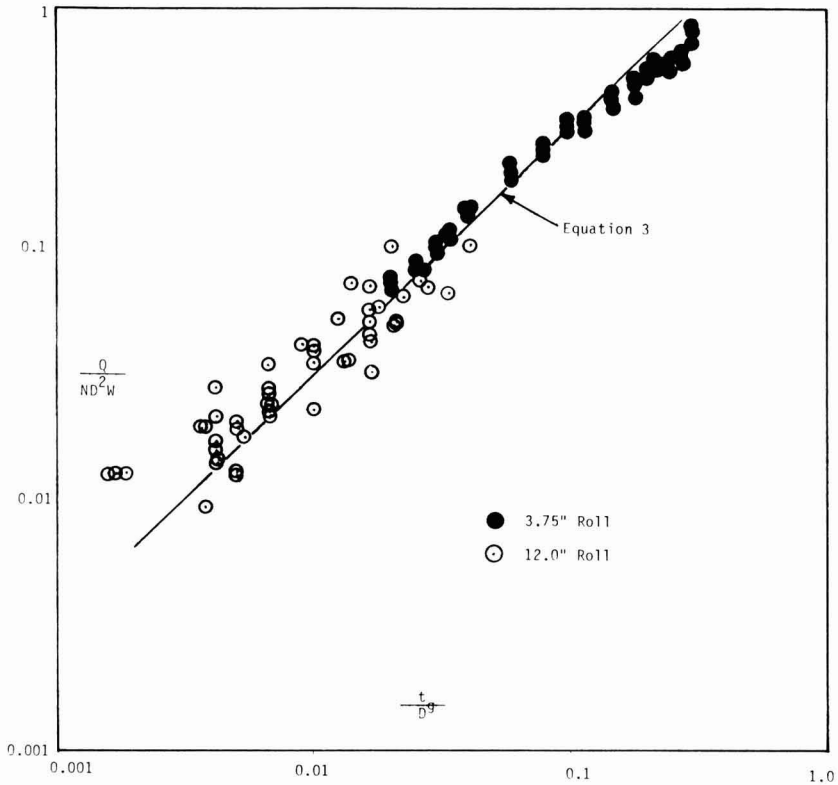
FIG. 7.   FLOW DATA PLOTTED ACCORDING TO EQ. 3.

An empirical approach to the problem yields better correlations. Dimensional analysis suggests (Eq. 11):

$$N_{P_o} = (N_{R_e}, \ t_f/t_g, t_g/D, n) \tag{11}$$

For this dough, we have searched for a correlation suggested by Eq. 11, namely (Eq. 12):

$$N_{P_o} = A(N_{R_e})^a \ (t_g/R)^b \ (t_f/t_g - 1)^c \tag{12}$$

Since, only one dough was studied, the effect of the flow index, n, on the correlation could not be determined. Regression yields the following Eq. 13 having a correlation coefficient (r^2) of 0.96.

$$N_{P_o} = 2.55 \ \left\{ \frac{1}{N_{R_e}} \left(\frac{t_g}{D} \right)^{1/3} \right\}^{1.77} \tag{13}$$
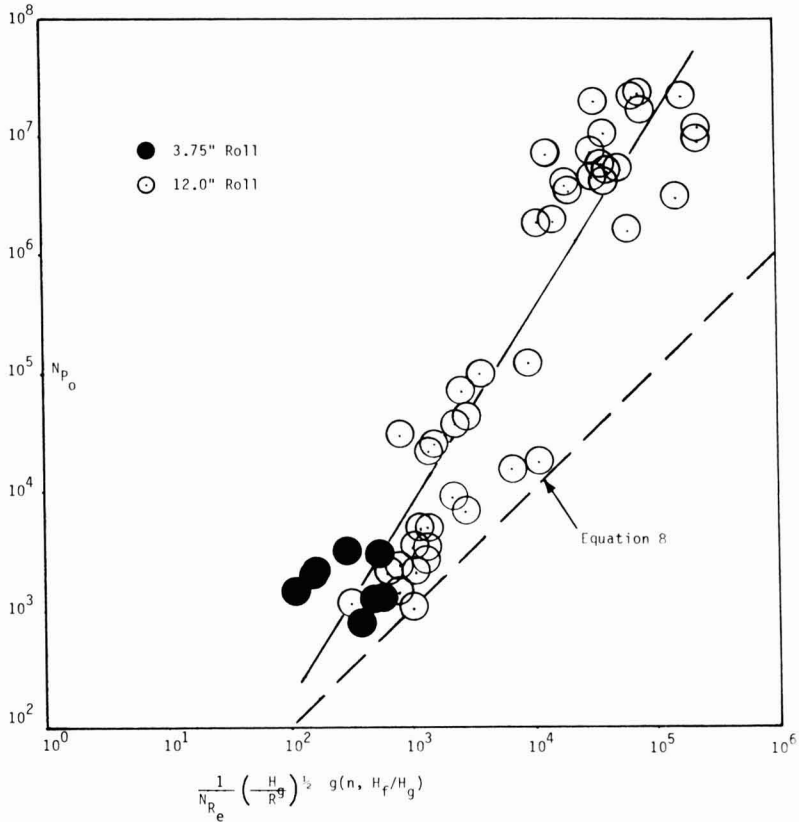
FIG. 8.   POWER DATA PLOTTED ACCORDING TO EQ. 8.

Figure 9 is a plot of the data in the form suggested by Eq. 13.

Surprisingly, the effect of feed thickness is unimportant. This would seem incorrect, but visual observation of the rolls provides an explanation.

Unlike the schematic representation of Fig. 3, deformation of the dough does not begin upon contact with the roll. Because of the solid-like nature of the dough, the rolls act on the dough far upstream from the actual roll contact point indicated in Fig. 3.

Actually, the dough drawn into the rolls assumes a shape as illustrated in Fig. 10. As a result, the roll contact point is much closer to the nip than has been assumed.

Despite the limitations of Eq. 13, its usefulness should not be overlooked. One equation clearly describes the performance of different sized rolls, which is the essence of the scale-up problem. For any particular dough, Eq. 13 can be developed with a small amount of energy expended in the pilot plant, and the results may be used to design or specify operating conditions of larger rolls.
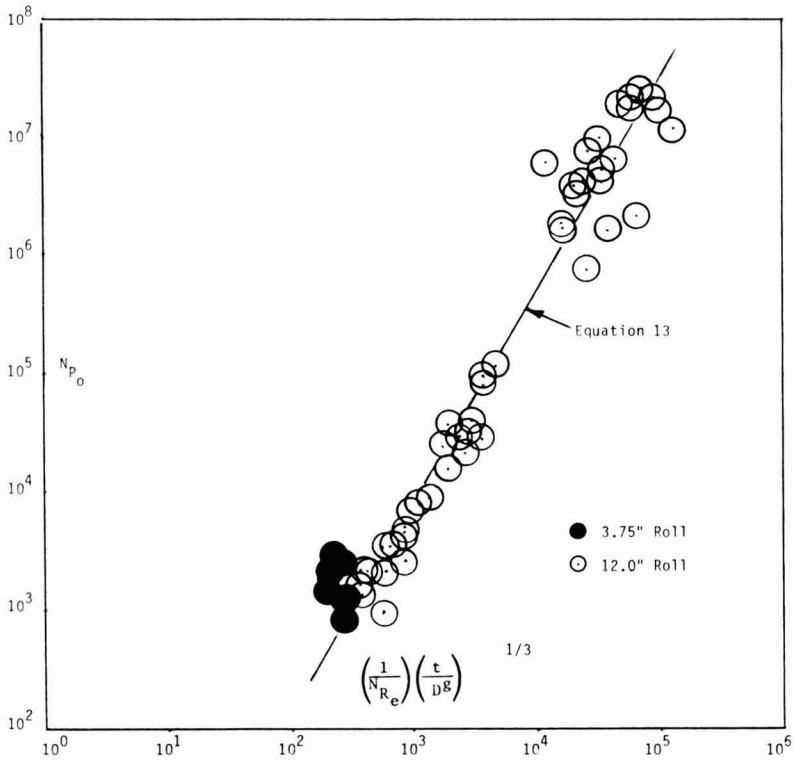
FIG. 9.   DATA PLOTTED ACCORDING TO EQ. 13.

The final area of performance which needs to be predicted is the actual final thickness of the dough obtained, since this dimension is almost always specified for a particular product attribute. Using dimensional analysis we will look for a correlation of the form (Eq. 14):

$$\frac{t_o}{t_g} = f \quad (t_f/D, \ t_g/D, N_{R_e}, n) \tag{14}$$

Since only one dough has been examined, the dependency of the correlation on the power law index is not definable. Regression analysis yields (Eq. 15):

$$\frac{t_o}{t_g} - 1 = 0.055 \left(\frac{t_g}{D}\right)^{-0.58} e^{27.4 \ N_{R_e}} \tag{15}$$

A correlation coefficient of 0.74 was obtained. The quality of the correlation suffers because of the difficulty of measuring dough thickness. Figure 11 is a plot of
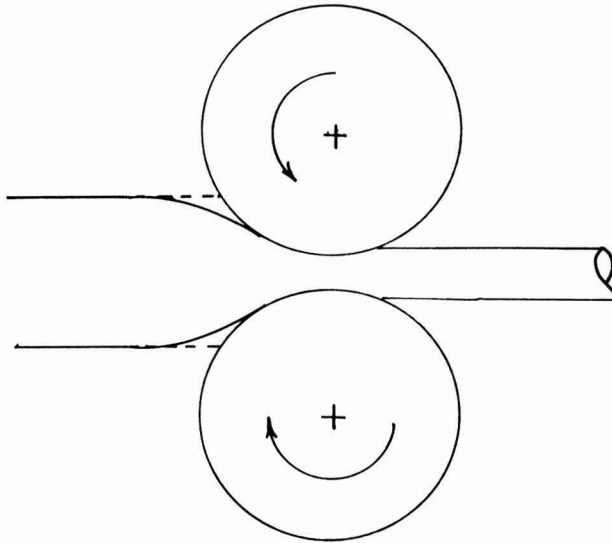
FIG. 10.   SCHEMATIC: TRUE REPRESENTATION OF DOUGH.

data in the form suggested by Eq. 15. Once again, one correlation describes both roll sizes. Note that at high Reynold's numbers and small roll spacing, the actual final thickness of the dough might be four times greater than the roll spacing.

Equations 4, 13 and 15 allow the specification of a series of rolls to reduce a dough to a specified final thickness at a specified production rate and energy input. The required calculation is quite cumbersome but possible. Rather than consider this task, it is far more informative to consider the effects of changing roll size and speed.

First let us consider the effect of roll size on the process. Assume that final desired sheet thickness is 1/8 in. To simplify calculation, we may approximate Eq. 15 in the range of interest as (Eq. 16):

$$\frac{t_o}{t_g} \simeq 0.06\left(\frac{t_g}{D}\right)^{-0.58} + 1 \tag{16}$$

Using Eq. 16, we can generate Table 1. This table illustrates that large diameter rolls require smaller gaps, to achieve the same product thickness as a small roll.

According to Eq. 4, this will require that the rolls be run at different speeds, and hence impart different energy inputs. Table 2 summarizes these calculations. The results listed in this table illustrate the type of problem one can encounter. Full scale rolls impart much more energy to the dough than the smaller diameter rolls typically used in the pilot plant or laboratory. As a consequence the performance characteristics of the two doughs will differ. One of two actions will be required.
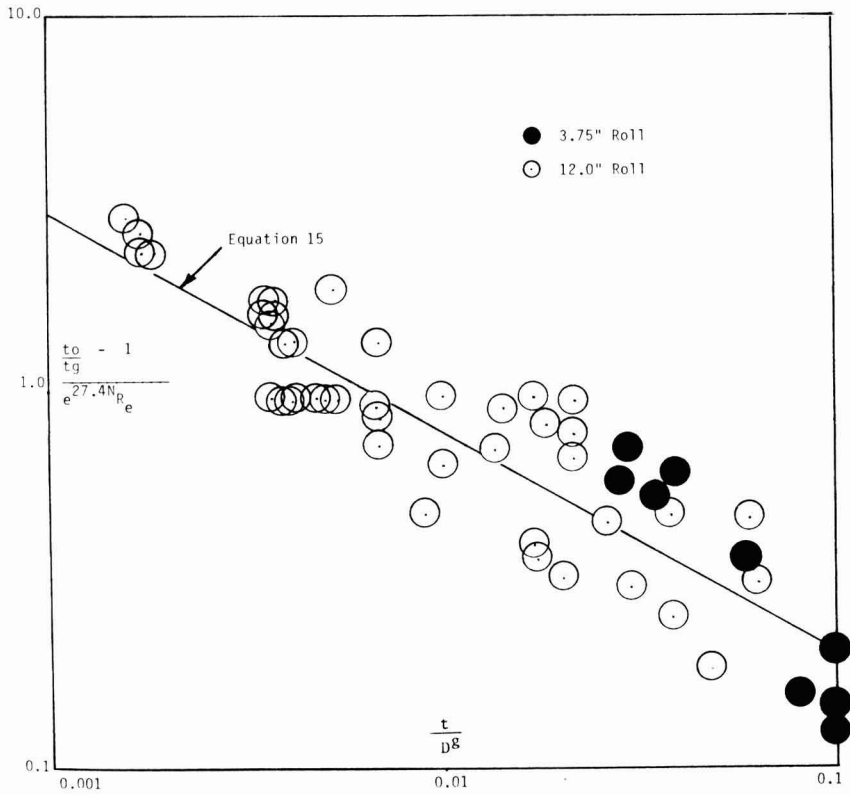
FIG. 11.   DATA PLOTTED ACCORDING TO EQ. 15.

Table 1.   Required roll diameter to attain at 1/8 in. sheet.

DIAMETER (in.)	GAP (in.)
3	0.085
4	0.079
6	0.070
8	0.062
12	0.052

Table 2.   Relative speeds and power consumption for various diameter rolls.

DIAMETER (in.)	RELATIVE ROTATIONAL RATE	RELATIVE POWER
3	1.00	1.00
4	0.81	1.18
6	0.59	1.49
8	0.52	1.83
12	0.41	2.42

Pilot plant rolls must be run at different conditions to anticipate plant behavior, or the dough will have to be mixed to a different degree of development to attain the same level of performance. Alternatively, one might be able to formulate doughs with a high degree of work tolerance.

CONCLUSIONS

The treatment of dough sheeting by simple theoretical models is insufficient for prediction of sheeter power consumption. The failure of the models is probably due to the complex nature of dough rheology. Empirical modification of the theoretical model yields a model which adequately predicts power consumption over a range of roll sizes and speeds for a particular dough. We can infer from these models that common pilot plant or laboratory procedures will not easily scale up to production equipment.

SYMBOLS

English

a,b,c = arbitrary constants
D = roll diameter
H = one half of sheet thickness
G = function defined by Eq. 8c
$h(x)$ = distance from centerline to roll surface
m = power law flow consistency
N = roll rotational speed
N_{P_o} = Power number

N_{R_e} = Reynold's number
n = power law flow index
P = power consumption
p = pressure between rolls
Q = volumetric dough rate
R = roll radius
t = sheet thickness
U = peripheral roll velocity
W = roll width
x = coordinate in direction of dough flow
$\tilde{x}$ = dimensionless position
y = coordinate in direction normal to dough flow

Subscripts

f = feed position
g = nip
o = output

Greek Letters

$\dot{\gamma}$ = shear rate (s^{-1})
λ = dimensionless distance from nip to separation
ϱ = dough density
T = shear stress (dynes/cm²)

REFERENCES

BERGEN, J. T. and SCOTT, G. W. 1951. Pressure distribution in the calendering of plastic materials, J. Appl. Mech., Trans. ASME, 73, 101.

BRAZINSKY, I., COSWAY, H. F., CLARK JONES, R. and STORY, V. 1970. Theoretical study of liquid film spread height in calendering of Newtonian and power law fluids. Apl. Polymer Sci. 2, 2771.

CHONG, J. S. 1968. Calendering thermosplastic materials, J. Appl. Polymer Sci. 12, 192.

CURRY, A., LEVINE, L. and ROSE, D. 1976. Method of forming rippled chip type products, U.S. Pat. #3,956,517.

ELIZAROV, V. I. and SIRAZETDINOV, T. K. 1973. Non-Newtonian Fluid in the Gap Between Rotating Cylinders, Izuestiya VUZ Aviatsionnaya Tekhnika 15, (4), 10.

FEILLET, P., FEVRE, E. and KOBREHEL, K. 1977. Modification in durum wheat protein properties during pasta dough sheeting, Cereal Chem. 54, (3), 580.

HALTON, P. and SCOTT BLAIR, G. W. 1937. A study of some physical properties of flour doughs in relation to their breadmaking qualities, Cereal Chem. *14*, 201.

HARPER, J. M. 1981. *Extrusion of Foods*, Vol. I, pp. 45, CRC Press, Boca Raton, Fla.

HUMMEL, C. 1950. *Macaroni Products*, Food Trade Press, London.

HLYNKA, I. 1962. Influence of temperature, speed of mixing, and salt on some rheological properties of dough in the farinograph, Cereal Chem. *39*, 286.

KILBORN, R. H. and TIPPLES, K. H. 1974. Implication of the mechanical development by means of sheeting rolls, Cereal Chem. *51*, (5), 648.

LAUNAY, B. and BURE, J. 1973. Application of a viscometric method to the study of wheat dough, J. Text. Stud. *4*, (1), 82.

LEIPA, A. 1977. Meat Analog, U.S. Pat. #4,001,441.

LEVINE, L. 1983. Estimating output and power of food extruders, J. Food Proc. Eng. *6*, (1), 1.

MATZ, S. A. 1968. *Cookie and Cracker Technology*, AVI Publishing Co., Westport, Conn.

MIDDLEMAN. S. 1977. *Fundamentals of Polymer Processing*, McGraw-Hill Book Co., New York.

MOSS, H. J. 1980. Strength requirements of doughs destined for repeated sheeting compared with those of normal dough Cereal Chem. *57*, (3), 195.

MULLER, H. G., WILLIAMS, M. V., RUSSEL EGGITT, P. W. and COPPOCK, J. B. 1961. Fundamental studies on dough with the Braebender extensograph, J. Sci. Food Agri. 12, 513.

SCHOFIELD, R. K. and SCOTT BLAIR, G. W. 1932. The relationship between viscosity, elasticity, and plastic strength as illustrated by some mechanical properties of flour dough, Proc. Roy. Soc. *138*, 707.

STENVERT, N. L., MOSS, R., POINTING, G., WORTHINGTON, G. and BOND, E. E. 1979. Bread production by dough rollers, Baker's Digest *22*, April.

WATANABE, Y. and MAGASAWA, S. 1968. A study on rheological properties of noodle by means of relaxation test, J. Food Sci. Techn. (Nihon Shokukin Kogyo Dakkai-Shi) 15, (10), 466.

CONSIDERATIONS IN CALCULATING KINETIC PARAMETERS FROM EXPERIMENTAL DATA

ABOLFAZL ARABSHAHI

Institute for Enzyme Research
University of Wisconsin-Madison
Madison, WI 53705

DARYL B. LUND

Department of Food Science
University of Wisconsin-Madison
Madison, WI 53706

ABSTRACT

Engineers require quantitative models to design and optimize processes. In the food industry, these process models become very complex because of the unique physical/chemical characteristics and variability of the raw material. Furthermore, frequently data describing rates of reactions and/or changes in foods are generated by food scientists who are not thoroughly familiar with reaction models. Analysis of those data to obtain parameters for reaction models thus becomes critical. In this paper, calculating kinetic parameters from experimental data is examined, and suggestions are presented for determining reaction rates and temperature dependence.

INTRODUCTION

In recent years, there has been increased interest in the application of kinetics to the loss of quality in foods during storage and processing (Lund 1983). This is in contrast to reporting end-point data which was common in early food science literature (Brenner *et al.* 1948; Guerrant and O'Hara 1953). Generally, rate of deterioration of a quality factor "*C*" can be represented by (Eq. 1):

$$dC/dt = -k(C)^n \qquad (1)$$

where dC/dt = disappearance of C per unit of time

k = rate constant

C = concentration of C at time t

n = order-of-reaction

Order-of-reaction can be determined by many different methods that are briefly discussed by Hill and Grieger-Block (1980). However, the time dependence for the majority of losses in food appear to be described by zero or first order models (Lenz and Lund 1980). Although a zero or first-order model describes concentration as a function of time, this does not mean that this represents the order of the mechanism of the reaction. Generally, the mechanism of many such reactions are very complex. Nonenzymatic browning reaction in dry food and enzymatic degradation of fresh fruits are examples of reactions described by a zero order model (Labuza and Kreisman 1978). Many other deteriorative reactions in food, such as loss of vitamins, microbial death, and rancidity in oils can be represented by a first-order model (Labuza and Kreisman 1978).

Since the order-of-reaction is merely used to provide a model for complex reactions, it is necessary to report all data pertaining to the conditions of the reaction. One of the most important initial conditions that is often not reported is this initial concentration of reactant. If, for example, a reaction is analyzed as zero-order $(dC/dt = -k_0)$ but the reaction is really first-order $(dC/dt = -k_1 C)$, then the rate constant k_0 is dependent on the concentration of reactant over the course of the reaction $(k_0 = k_1 C)$. The reaction appears zero-order only because the extent of reaction is small $(C_t \simeq C_0)$. If the experiment were conducted at a different initial concentration a different rate constant would be obtained. Where possible reactions should be followed through at least 4-5 half-lives $(C_{final} \leq 0.07 \ C_{initial})$.

A common procedure for analyzing and reporting data that can be modeled by a first order reaction includes: (1) calculating the rate constant (k) by linear regression analysis of the logarithm of retention of ''C'' vs time, (Other indices proportional to concentration such as height of peaks in a chromatogram can be used for this purpose) and (2) determining the Arrhenius activation energy (E_a) using regression analysis of log of rate constant vs reciprocal of absolute temperatures $(1/T)$. In many cases there is no consideration for the statistical variance associated with the kinetic parameters.

Two common mistreatments of kinetic data are: (1) using relative retention or percent retention instead of raw data to determine the rate constant. There is an uncertainty in the initial concentration that is often at least the same order of magnitude as uncertainty in other observed concentrations. Therefore, it is not appropriate to divide all observations by the average value of the measured initial concentration, (2) the variability in rate constants is generally ignored in calculation of activation energy.

Given these inconsistencies in treating kinetic data, it is the purpose of this paper to present some methods of analyzing kinetic data which provide statistically more reliable final results. Two cases will be considered: (1) calculating rate constants and (2) calculating Arrhenius activation energy. Although the examples are for a first-order kinetic model, the considerations apply to any order kinetic model.

CALCULATING RATE CONSTANTS

First, for rate constant determination, raw data should be used in Eq. 2 when the initial concentration is not accurately known, which is usually the case.

$$ln \ C = ln \ C_0 \ - \ kt \tag{2}$$

Performing regression analysis on Eq. 2 provides information on both the intercept and slope. Adequacy of the model is based on the sum of squares of residuals, coefficient of determination (R^2), visual examination of distribution of residuals, lack of fit test, and a plot of the data.

The residuals, which are differences between observed values and values predicted by the regression equation, can be thought of as the observed errors if the model is correct (Draper and Smith 1966). Therefore, the residuals should be randomly distributed about zero when a proposed model is correct. In analyzing data of concentration versus times, one should be cautious when the logarithmic form of the first order kinetics equation ($ln \ C = ln \ C_0 \ - \ kt$) is used rather than the exponential form ($C = C_0 e^{-kt}$). The logarithmic transformation may result in an increased variance with time even though the distribution of residuals for the exponential model do not show a pattern. If the logarithmic transformation introduces a pattern to the distribution of residuals, then nonlinear regression using the exponential form of the model is more appropriate, or a weighted least squares analysis should be used (Neter and Wasserman 1974). If this patterned distribution of residuals is observed after unweighted regression, the inverse of the square of residuals from this first regression can be used as a weight for a second regression (Hill and Grieger-Block 1980).

Data on thiamin concentration as a function of time in an intermediate moisture model system containing propylene glycol, riboflavin and niacin stored in TDT cans at different temperatures are given in Table 1 (Arabshahi 1982). Figure 1 shows a comparison of distribution of residuals for data of thiamin retention (nitrogen flushed, stored at 25 °C, Table 1) with (a) unweighted linear regression and (b) weighted linear regression where the inverse of the square of residuals was used as the weight factor. It can be seen that using an unweighted regression resulted in a skewed distribution of residuals (a) indicating that the model is not adequate. On the other hand, using weighted regression resulted in an unskewed distribution of residuals (b) indicating the model is adequate. Using weighted regression did not change the rate constant but the standard deviation of the rate constant decreased by an order of magnitude.

Frequently nonlinearity is observed in the plotted data of nutrient retention versus time, especially at the beginning of the experiment. Figure 2 represents a hypothetical example. The deviation from a straight line might be caused by inadequacy of the model or a time lag during the early stage of reaction. If the investigator suspects that a first-order model is still sufficient, it is essential that an appropriate correc-

Table 1.   Thiamin concentration as a function of time in an intermediate-moisture model system
containing propylene glycol[a,b] (a_w=0.75 @ 20° C[c]).

Temperature (°C)	Time (days)	Thiamin Concentration ($\mu g/g_{solid}$)[d,e] in Cans Flushed with:		
		Nitrogen	Air	Oxygen
25	31	61.6 (+ 1.8)	65.9 (+ 1.8)	61.1 (+ 2.1)
	62	60.2 (+ 1.6)	56.1 (+ 2.0)	60.3 (+ 0.4)
	91	53.9 (+ 1.7)	54.6 (+ 1.1)	56.7 (+ 1.7)
	122	46.9 (+ 1.9)	47.8 (+ 1.5)	47.9 (+ 1.1)
	152	48.1 (+ 1.8)	46.3 (+ 1.7)	47.1 (+ 0.5)
	197	39.8 (+ 1.7)	37.8 (+ 1.5)	42.7 (+ 1.5)
	257	32.2 (+ 1.6)	34.9 (+ 1.3)	34.4 (+ 1.5)
35	31	48.9 (+ 1.9)	49.0 (+ 1.6)	50.5 (+ 1.4)
	62	43.8 (+ 1.7)	44.9 (+ 1.4)	42.7 (+ 1.1)
	91	38.7 (+ 2.0)	37.5 (+ 1.2)	39.2 (+ 1.3)
	122	32.4 (+ 1.3)	33.9 (+ 1.0)	33.0 (+ 1.7)
	152	24.1 (+ 1.1)	24.2 (+ 1.2)	23.5 (+ 0.3)
45	31	32.9 (+ 2.0)	31.9 (+ 1.8)	31.1 (+ 1.5)
	62	17.2 (+ 1.2)	15.7 (+ 1.3)	19.0 (+ 2.2)
	91	7.1 (+ 2.0)	8.7 (+ 1.2)	7.0 (+ 1.3)
55	3	55.5 (+ 2.2)	53.3 (+ 2.1)	56.2 (+ 1.5)
	7.25	35.2 (+ 1.6)	32.8 (+ 1.3)	33.8 (+ 1.5)
	11.1	25.3 (+ 1.4)	25.4 (+ 2.1)	24.7 (+ 1.6)
	19	9.1 (+ 1.4)	10.5 (+ 1.3)	9.9 (+ 0.7)

[a]From Arabshahi (1982).

[b]The model system contains microcrystalline cellulose, propylene glycol, sodium
propionate, thiamin, riboflavin, niacin and water.

[c]a_w = 0.77 @ 25°C, 0.79 @ 35°C, 0.81 @ 45°C, 0.82 @ 55°C.

[d]Measured thiamin concentration at zero times was 70.1 g/g solid with a standard
deviation of 1.36.

[e]Average of two replicates ($\pm$ range).

tion be made for this time lag, especially when the time lag is not sufficiently small
relative to the half life of the reaction. Time lags may occur as a result of some
changes in internal or external conditions of the reaction. Frequently, a change in
temperature during initial equilibration of the sample is responsible for the time lag.

The lag time can be accounted for in the calculation of the rate constant by ex-
cluding data obtained in the lag period. Deciding what portion of kinetic data should
be excluded is critical. Neter and Wasserman (1974) suggest the following rule for
deciding whether an extreme or outlier value should be discarded: an extreme obser-
vation can be discarded when there is some evidence that this extreme value is the
result of a mistake or other extraneous effects and also if this extreme observation
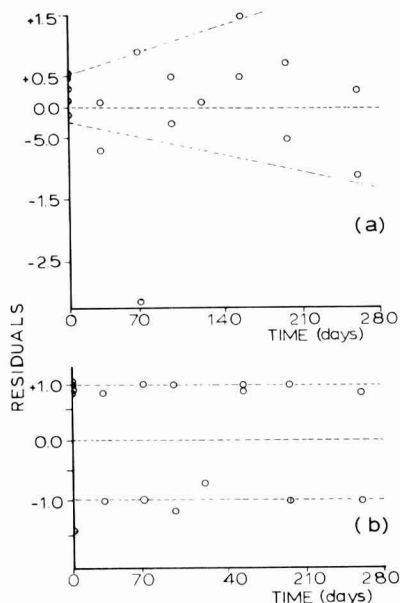
FIG. 1.   PLOTS OF RESIDUALS OF THIAMIN RETENTION DATA IN AN INTERMEDIATE
MOISTURE MODEL SYSTEM (NITROGEN FLUSHED) AT 25° C:
   a. unweighted linear regression.
   b. weighted linear regression.

(from Arabshahi 1982)

has a large standardization residual. The standardization residuals are the residuals
divided by an estimate of their standard deviation. The most usual standardized
residuals varies between -2 and $+2$ (Ryan *et al.* 1976).

   Visual examination of Fig. 2 shows an initial deviation from linearity. After per-
forming linear regression, this deviation was also evident from the value of the stan-
dardized residual which was greater than 2 for observation at zero time. A second
regression was performed after omitting the observation at zero time from the data.
The results of this regression included a standardized residual greater than 2 for
concentration after 5 min. After omitting the datum corresponding to 5 min., a third
regression was performed. The result of this final regression does not include a stand-
ardized residual value out of the normal range. Table 2 shows the results of these
three regressions. It can be seen that omitting the extreme values from the data set
based on the recommendation of Neter and Wasserman (1974) improved the R^2 value
from 98.2 to 99.9 and reduced the standard deviation of the rate constant from 0.0011
to 0.00012.

   In addition to the rate constant, regression analysis of kinetic data provides an
estimate of the initial concentration (C_0). Provided the model describes the data suf-
ficiently, this estimated value for initial concentration is more reliable than the average
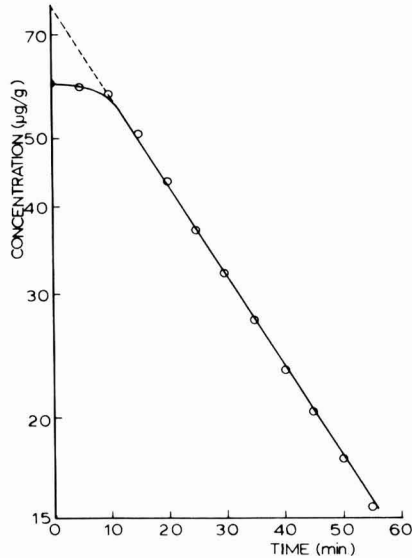
FIG. 2.   CONCENTRATION VERSUS TIME FOR HYPOTHETICAL DATA WHEN THERE IS
         A TIME LAG.

of measured replications of initial concentration because observed concentrations at different time intervals have some information about initial concentration. When several experiments have been performed all starting at the same initial concentration, the initial concentration for the whole set may be estimated more accurately by performing a multiple linear regression with the model (Eq. 3):

$$ln \; C_j = ln \; C_0 - k_1 t_{1i} - k_2 t_{2i} - \ldots - k_n t_{ni} \tag{3}$$

The estimated rate constants for data of Table 1 using two different methods of analysis (multiple linear regression and individual linear regression) are shown in Table 3. It can be seen that there are differences between mean values of the rate constant at the same temperature estimated by different methods of analysis, although in this case the differences are not statistically significant at the 95% confidence level. These differences arise because of a basic assumption about the experimental conditions. In one case, it was assumed that initial concentrations at different temperatures are the same, and in the other case it was assumed initial concentrations might be different.

CALCULATING ACTIVATION ENERGY

The temperature dependence of most reactions in foods can be expressed by the Arrhenius model. Frequently investigators apply linear regression analysis to the

Table 2. Hypothetical kinetic data and its rate constant.

Time (min)	Concentration ($\mu g/g$)	Standardized Residuals from Linear Regression		
		1st	2nd	3rd
0	60.0	-2.68		
5	59.0	-0.63	-2.97	
10	58.0	1.25	0.92	-1.55
15	50.5	1.18	1.04	1.06
20	43.5	0.96	0.88	1.30
25	37.0	0.40	0.40	-0.86
30	32.0	0.42	0.37	0.19
35	27.5	0.19	0.18	0.03
40	23.5	-0.14	-0.17	-1.20
45	20.5	-0.16	0.04	1.53
50	17.5	-0.53	-0.37	0.06
55	15/-	-0.87	-0.69	-0.70
$k(min^{-1})$		0.0271	0.0289	0.0301
Std. dev of k (min-1)		0.0011	0.00074	0.00012
R^2		98.2	99.4	99.9
Degrees of freedom		10	9	8

mean value of the rate constants (k) ignoring the variability of each k value even though this variability in k is usually calculated. The appropriate approach is to incorporate this variability in the rate constant by using weighted regression analysis with the inverse of the variance of $ln\ k$ as regression weights (Box *et al.* 1978). An estimate of the variance of $ln\ k$ can be determined from (Young 1962) (Eq. 4):

$$(SD_{ln\ k})^2 \ = \ (1/k)^2(SD_k)^2 \tag{4}$$

where $(SD_{ln\ k})^2$ = variance of $ln\ k$

k = rate constant

$(SD_k)^2$ = variance of k

Thus weights for the linear regression of the Arrhenius equation in linear form are $k^2/(SD_k)^2$. These weights have the effect that a k value with a larger standard deviation carries less weight in regression and vice versa. If the standard deviation for the rate constants are approximately equal, unweighted regression analysis may be applied.

For calculating the Arrhenius activation energy (E_a), the method previously

Table 3. Rate constants and initial concentrations[a] for thiamin degradation in a model system containing propylene glycol sealed in TDT cans ($a_w = 0.75$ @ $20°$ C[b]).

Gas in TDT Cans	Temper- ature (°C)	Individual Linear Regressions		Multiple Linear Regression	
		Initial Concen. (μg/g solid)	k (Std. dev.) (day^{-1})	Initial Concen. (μg/g solid)	k (Std. dev.) (day^{-1})
Nitrogen	25	68.72	0.0028 (0.00022)	70.11	0.0029 (0.00017)
	35	67.36	0.0066 (0.00034)	"	0.0068 (0.00028)
	45	71.52	0.0249 (0.0013)	"	0.0247 (0.00055)
	55	72.97	0.106 (0.0024)	"	0.103 (0.0027)
Air	25	70.11	0.0028 (0.00012)	"	0.0028 (0.00017)
	35	68.03	0.0065 (0.00035)	"	0.0068 (0.00028)
	45	68.72	0.0233 (0.00076)	"	0.0235 (0.00055)
	55	70.81	0.099 (0.0034)	"	0.098 (0.0027)
Oxygen	25	70.11	0.0026 (0.00011)	"	0.0026 (0.00017)
	35	68.03	0.0066 (0.00033)	"	0.0069 (0.00028)
	45	70.81	0.0244 (0.0013)	"	0.0242 (0.00055)
	55	72.24	0.102 (0.0027)	"	0.100 (0.0027)

[a]Measured initial concentration at zero time was 70.1 μg/g$_{solid}$ with a standard deviation of 1.36.

[b]a_w = 0.77 @ 25°C, 0.79 @ 35°C, 0.81 @ 45°C, 0.82 @ 55°C.

discussed consists of two steps: (1) regressing concentration on time at constant temperature to determine the rate constant, k, and (2) regressing $ln\ k$ on reciprocal temperature to determine E_a. Generally this two-step procedure results in a relatively large standard deviation in E_a and particularly with a large confidence interval caused by the small number of degrees of freedom. To increase the degrees of freedom, thus narrowing the confidence interval, the following equation was derived to calculate activation energy directly from original data in one step.

Assume there are N sets of data (concentration versus time) that are for the same reaction at N different constant temperatures ($T_1, T_2, \ldots, T_N$). Each set of data has n_i observations ($i = 1,N$) that correspond to n_i time intervals (t_{ij}). Totally there are $\sum_{i=1}^{N} n_i$ observations with the numbers of the set denoted as $C_{(t_{ij}, T_i)}$ where $i = 1,2, \ldots, N$ and $j = 1,2, \ldots, n_i$. A first order model for the data at each temperature T_i can be written (Eq. 5):

$$C_{(t_{ij}, T_i)} = C_{0(T_i)} * \exp(-k_{(T_i)}t_{ij}) \tag{5}$$

where $C_{(t_{ij}, T_i)}$ = concentration of C at time t_{ij} and temperature T_i

$C_{0(T_i)}$ = initial concentration at time zero for temperature T_i.

Incorporating the Arrhenius equation into equation 5 results in (Eq. 6):

$$C_{(t_{ij}, T_i)} = C_{0(T_i)} \exp[-k_0 t_{ij} \exp(-E_a/RT_i)] \tag{6}$$

This is a nonlinear model in $(N + 2)$ parameters:

$$C_{01}, C_{02}, C_{03} \ldots C_{0N}, k_0, E_a.$$

This nonlinear regression can be performed with any nonlinear regression package. In this case, the BMDP3R computer program was applied to data on retention of thiamin. The following manipulations were performed to speed up convergence of the program.

Let $X_i = 1/RT_i$, $\bar{X} = 1/N \sum\limits_{i=1}^{N} X_i$, and

$\theta = k_0 \exp[-E_a\bar{X}]$. After substitution, Eq. 6 becomes (Eq. 7):

$$C_{(t_{ij}, T_i)} = C_{0(T_i)} \exp\left\{-\theta t_{ij} \exp[-E_a(X_i - \bar{X})]\right\} \tag{7}$$

where θ is a new parameter, X_i is a new variable, and $\bar{X}$ is a new known constant. For BMDP3R, the model was written in the following form (Eq. 8):

$$y = P(I)*\exp\left\{-P(N + 1)*t*\exp[-P(N + 2)(X_i - \bar{X})]\right\} \tag{8}$$

where $I = 1, 2, \ldots, N$. Partial derivatives of Equation 8 with respect to parameters are:

$$\frac{\partial y}{\partial\, P(I)} = \exp -P(N + 1)*t*\exp[-P(N+2)*(X_i - \bar{X})]$$

$$\frac{\partial y}{\partial\, P(N + 1)} = -t \exp[-P(N + 2)*(X_i - \bar{X})]*y$$

$$\frac{\partial y}{\partial\, P(N + 2)} = \frac{\partial y}{\partial\, P(N + 1)} * P(N + 1)*(\bar{X} - X_i)$$

Table 4. Arrhenius activation energies for thiamin degradation in intermediate-moisture model systems, estimated by two different methods[a].

Model System	a_w[b]	Two-step method				One-step method			
		E_a (Kcal/mol)	Degrees of freedom	Std. dev. of E_a (Kcal/mol)	95% confidence interval	E_a (Kcal/mol)	Degrees of freedom	Std. dev. of E_a (Kcal/mol)	95% confidence interval
1c	0.75	29.1	1	2.5	-2.9 to 61.1	26.8	20	0.87	25.0 to 28.6
2d	0.75	24.3	2	2.1	15.3 to 33.3	23.9	113	0.41	23.1 to 24.7
3e	0.65	25.8	1	1.9	1.7 to 49.9	25.7	27	1.4	22.8 to 28.6
	0.75	27.0	1	2.4	-3.0 to 57.0	27.1	27	1.5	24.1 to 30.1
	0.85	28.0	1	2.3	-0.7 to 56.7	28.3	27	1.6	25.1 to 31.5
4f	0.65	23.0	1	0.97	10.7 to 35.3	23.1	22	1.3	20.5 to 25.7
	0.75	24.5	1	1.2	8.7 to 40.3	24.1	22	1.5	21.0 to 27.2
	0.85	25.7	1	1.5	6.6 to 44.8	25.4	22	1.4	22.4 to 28.4

aFrom Arabshahi (1982).
bAt 20°C.
cContains microcrystalline cellulose, propylene glycol, sodium propionate and thiamin.
dContains microcrystalline cellulose, propylene glycol, sodium propionate, thiamin, riboflavin and niacin.
eContains microcrystalline cellulose, glycerol, sodium propionate, and thiamin.
fContains microcrystalline cellulose, polyethylene glycol-400, sodium propionate, and thiamin.

This method was applied in a study by Arabshahi (1982). Stability of thiamin in an intermediate moisture model systems as a function of time, temperature, oxygen, a_w, humectant, and moisture content was studied. Table 1 is an example of data obtained in this study. Using data reported in Table 1 and also data on thiamin concentration as a function of time, temperature and a_w in other model systems (not reported here), activation energies for thiamin degradation in four different model systems were estimated by this one-step method. For data in Table 1 (model system 2), it was concluded that oxygen concentration did not have a significant effect on rate of degradation, and thus data on thiamin concentration as a function of time in different atmospheres were treated as replicate data.

Activation energies estimated by the one-step method and by the two-step method are reported in Table 4. Based on the lack of fit test and examination of residuals, it was concluded that the model used for the one-step method was adequate for data sets corresponding to the different model systems. When the log form of Eq. 8 was applied as a model for the one-step method, the plots of residuals were patterned indicating that the assumption of constant variance of errors did not apply. Therefore, the exponential form (Eq. 8) was used.

It can be seen in Table 4 that, with the exception of the E_a value calculated for model system 2, the E_a value calculated by the one-step method was within one kcal/mol of that obtained by the two-step method. There was no consistent trend as to which method gave the largest value. Generally, however, the standard deviations estimated by the one-step method are smaller than those estimated by the two-step method, and in all cases the 95% confidence intervals estimated by the two-step method are much larger than those estimated by the one-step method. A comparison of activation energies calculated from the two-step method is virtually meaningless because of the extremely large confidence intervals. However, a comparison based on E_a calculated from the one-step method could be meaningfully interpreted because of the smaller confidence intervals. Although it was not used in this study, the resulting equation for a one-step method for a zero-order model is (Eq. 9):

$$y = P(I) - P(N + 1)*t*\exp[-P(N + 2)*(X_1 - \bar{X})]$$

where P = parameter   (9)

I = 1,2, . . . ,N

CONCLUSION

To improve estimation of kinetic parameters and to provide more complete utilization of raw data, the following points should be considered:

(1) For rate constant determination, actual concentration data should be used rather than the fraction (or percent) remaining concentration. This avoids the uncertainty introduced by dividing all concentration values by the initial concentration which often has an uncertainty associated with it at least the same order of magnitude as the uncertainty in measured concentration at different time intervals. In addition to estimation of the rate constant, the proposed regression analysis provides an estimation of the initial concentration. When several experiments are performed with the same initial concentration, this common initial concentration can be estimated more accurately by performing a multiple linear regression.

(2) In treating kinetic data, care should be exercised when the logarithmic form of the first-order kinetics equation rather than the exponential form is used. The log transformation may introduce a trend in the residuals. If the logarithmic transformation introduces a pattern to the distribution of residuals, then a weighted least squares analysis should be used.

(3) The statistical variability in rate constant should be incorporated into calculation of activation energy. It is recommended that weighted regression analysis be used with the inverse of variance of "$ln\ k$" as regression weights.

(4) To calculate activation energy, a one-step method is proposed. Although the two-step method has the advantage of being simple, the proposed one-step method gives a smaller confidence interval than that estimated by the two-step method because there is a more complete utilization of raw data for estimating activation energy and initial concentration. Therefore, the application of the one-step method is recommended when the confidence interval on the kinetic parameters is statistically meaningless. Applying the one-step method could result in a reduced interval so comparisons of kinetic parameters can be made.

ADKNOWLEDGMENT

REFERENCES

ARABSHAHI, A. 1982. Effect and interaction of environmental and composition variables on stability of thiamin in intermediate moisture model systems. Ph.D. thesis. University of Wisconsin-Madison.

BOX, G. E. P., HUNTER, W. G. and HUNTER, J. S. 1978. *Statistics for Experimenters*: An introduction to design, data analysis, and model building. John Wiley and Sons, New York.

BRENNER, S., WODICKA, V. O. and DUNLAP, S. G. 1948. Effect of high temperature storage on the retention of nutrients in canned foods. Food Technol. 2, 207.

DRAPER, N. R. and SMITH, H. 1960. *Applied Regression Analysis*. John Wiley and Sons, New York.

GUERRANT, N. B. and O'HARA, M. B. 1953. Vitamin retention in peas and lima beans after blanching, freezing, processing in tin and glass, after storage and cooking. Food Technol. *7*, 473.

HILL, C. G. and GRIEGER-BLOCK, R. A. 1980. Kinetic data: generation, interpretation, and use. Food Technol. *34* (2), 56.

LABUZA, T. P. and KREISMAN, L. N. 1978. Open shelf life dating of foods. Contract Report Vol. 1. Office of Technology Assessment, Washington, DC.

LENZ, M. K. and LUND, D. B. 1980. Experimental procedures for determining destruction kinetics of food components. Food Technol. *34* (2), 51.

LUND, D. B. 1983. Considerations in modelling food processes. Food Technol. *37*(1), 92.

NETER, J. and WASSERMAN, W. 1974. *Applied Linear Statistical Models, Regression, Analysis of Variance, and Experimental Designs*. Richard D. Irwin, Inc., Homewood, IL.

RYAN, T. A., JOINER, B. L. and RYAN, B. F. 1976. *Minitab Student Handbook*. Duxbury Press, North Scituate, MA.

YOUNG, H. D. 1962. *Statistical Treatment of Experimental Data*. McGraw-Hill Book Co., New York.

USE OF TIME-TEMPERATURE DATA DURING FLUIDIZED BED FREEZING TO DETERMINE FROZEN FOOD PROPERTIES

M. MARIN[1], G. M. RIOS[2] and H. GIBERT[1]

[1]*Group d'étude des Procédés de l'Industrie Chimique et Agro-Alimentaire, Institut du Génie Chimique, 31078 Toulouse, France*

[2]*Laboratoire de Génie Chimique-Université des Sciences et Techniques du Languedoc, Place E. Bataillon 34060, Montpellier, France*

ABSTRACT

Most of the methods proposed in literature for freezing time calculation require the previous knowledge of the enthalpy change and thermal conductivity of frozen materials. Ordinarily these properties are not easy to obtain, and often need a special approach depending on the process under consideration.

This paper deals with a new and simple method that affords an estimation for Fluidized Bed Freezing of small food pieces (20-40 mm) immersed in a cold fluidized bed of fine inert particles. Based upon Plank equation and temperature-time recordings, the method more particularly yields the latent heat to be removed for bringing the product below the freezing point and the thermal conductivity of the matter in this final state. The associated percentage of water actually frozen during operation may be also determined.

With the help of this technique properties have been determined for various fruits and vegetables (banana, carrot, potato, turnip and cucumber). The values that have been found agree well with literature data: latent heats correspond to the latent heat required to freeze 80% of the water in the products, and thermal conductivities lie between 1 and 2 W/m°C. Helpful correlations for Fluidized Bed Freezing time calculation are proposed that simply relate these properties to the total water content of materials.

INTRODUCTION

Recently (Marin *et al.* 1983) a new technique for Individually Quick Frozen food production has been presented where a bubbling gas fluidized bed of small particles kept at low temperature freezes the foods immersed in it by direct contact. The pro-

cess has been shown to offer major advantages with low gas velocity requirement, homogeneous temperature of cooling medium, uniform exchange conditions on the whole external surface of products, high heat transfer coefficients (200 to 300 W/m²°C) and low water losses of food stuffs.

In the course of this work attempts have been made for predicting freezing times. Two simple methods have been more especially investigated: (1) the calculation from Plank equation, leading to times hereinafter referred to as t_P-values and (2) the graphical determination from "product core temperature against time "curves, leading to times hereinafter referred to as t_G-values. Experiments carried out with high water content products ($\geqslant 70\%$) have shown that the relative gap between t_G and t_P is fairly small (to the worse 20%) as long as (Eq. 1 and 2):

$$1 \leqslant Bi \leqslant 6 \tag{1}$$

$$\frac{T_o - T_f}{T_i - T_f} \leqslant 2 \tag{2}$$

with T_o the outside cooling medium temperature, T_f the freezing temperature, T_i the initial product temperature and Bi the Biot number (Marin 1982).

Based on this fact a new and quite interesting method for estimating effective properties of frozen foods during Fluidized Bed operations has been proposed. That is the main purpose of this paper to expose its basic principles and to present some typical applications.

METHODS

As it appears from literature (Charm 1971; Heldman 1975) a simple tool often used to predicting freezing times is the so-called Plank model. Derived from the four following assumptions: (1) at $t = 0$ the product is at freezing point with a uniform temperature equal to T_f, (2) the outside medium temperature T_o is constant, (3) the transfer of the latent L takes place at T_f and (4) the thermal conductivity λ and the density ϱ of frozen material are constant, this model leads to the well-known equation (Eq. 3):

$$t_p = \frac{\varrho \cdot L}{T_f - T_o} \cdot \left[P \cdot \frac{a}{h} + R \cdot \frac{a^2}{\lambda} \right] \tag{3}$$

with h the bed-to-object heat transfer coefficient, a the product thickness, P and R two dimensionless constants that depend on the product shape. As an example for spheres: $P = 1/6$ and $R = 1/24$. As reminded by Heldman (1975) there are serious limitations to this approach: (1) the procedure utilizes the initial freezing

point of the product in the computation equation and neglects the time required to remove sensible heat above the freezing point; (2) a constant thermal conductivity must be assumed for the frozen region and (3) the assumption is made that the food products will freeze in a manner similar to an ideal liquid. But most of the time the benefits of a compact and quite easy to use equation more than compensate for the slight inaccuracies involved in the computations.

As shown elsewhere (Marin 1982) operating times may be also determined from "product core temperature against time" curves. Such graphs, as simply recorded by means of immersed thermocouples, have standard shapes and they may be roughly regarded (Fig. 1) as composed of three linear segments: (1) AB associated to the rapid refrigeration of the material from the initial temperature T_i to the initial freezing level T_f ; (2) BC that is supposed to represent the properly so-called freezing step, in the course of which temperature does not vary too much and (3) CD corresponding to the next cooling down of the frozen product to the stocking temperature T_s. From them freezing times are deduced through (Eq. 4):

$$t_G = t_C - t_B \tag{4}$$

Undoubtedly there are numerous impediments to this approach (the measurement of the product core temperature as a function of time is very sensitive to accurate location of the temperature sensor; it is often difficult to determine the location of points B and C . . .) which make necessary special precautions to be taken for experiments.

For Fluidized Bed Freezing, operating characteristics are quite similar to the assumptions of Plank model with a constant cooling medium temperature and uniform heat transfer conditions all over the product surface. Moreover in the special working conditions delineated by Eq. 1 and 2, the preliminary refrigeration step of the material from T_i to T_f proves to proceed quickly and uniformly, low Biot numbers being responsible for high cold penetration rates and chosen temperature differences promoting at first the removal of sensible heat from the food core rather than the freezing of peripheric layers (Marin 1982). These facts are the origin of the tight relationship between t_P and t_G values.

So under such circumstances it may be written with a good accuracy (Eq. 5):

$$\frac{1}{v_G} = \frac{t_G}{a} \cdot 2 = \left[\frac{2\varrho L}{T_f - T_o} \cdot \frac{R}{\lambda} \right] a + \left[\frac{2\varrho L}{T_f - T_o} \cdot \frac{P}{h} \right] \tag{5}$$

and a quick estimation of the enthalpy change at freezing step associated to the latent heat removal L, as well as the calculation of the thermal conductivity of frozen material, appear to be possible from the analysis of "$1/v_G$ against a" curve characteristics.

EXPERIMENTAL DETAILS

The pilot plant has been thoroughly described elsewhere (Marin *et al.* 1983). So we shall just indicate here the fine particle and biological product characteristics as well as the bed operating conditions.

The fine particles in the freezing unit are glass beads of 630-710 μm. The gas velocity three times greater than the minimum fluidization rate ($U_{mf} = 35$ cm/s) insures a good mixing of the powder. Then a uniform treatment for the immersed body results with a surface heat transfer coefficient equal to 200 W/m² °C (Marin *et al.* 1983).

The experimental work has been conducted with potatoes, carrots, bananas, turnips and cucumbers spherically shaped and 20 to 40 mm in size. Such dimensions have been selected in order to satisfy Eq. 1. Indeed from literature it may be thought at first that λ values will not be far from 1 W/m°C (Heldman 1975; Charm 1971).

Most of the runs were carried out with products taken at room temperature ($T_i = 18$ °C) and then plunged into a cooling medium at about -40 °C. But with potatoes a few experiments were also realized at initial temperatures in the range between 18 and 80°C. Whatever the case, Eq. 2 was verified.

The values of the total water content w, of the initial freezing temperature T_f and of the frozen density of the foods ϱ were determined in a preliminary step of the study. They are reported in Table 1 and show to agree well with literature data (Heldman 1975; Fennema *et al.* 1973)

RESULTS

The various "temperature against time" curves obtained with the five products all exhibit a nearly horizontal *BC* line as shown in Fig. 1. This suggests that the freezing temperature does not vary too much for the high water content products here investigated. This fact constitutes a strong argument on behalf of the approach previously proposed, that makes the assumption that foods freeze in a manner similar to ideal liquids. Moreover from these graphs the determination of *B* and *C* points appears to be quite easy.

It must be also noted that all the experiments carried out at different initial product temperatures have led to t_G-values equal to better than ±5%, well in the frame of the proposed theory.

As an example the "$1/v_G$ against a" curves for potatoes and carrots have been plotted on Fig. 2 and 3. In good accordance with Eq. 5 the points are seen to fall into straight lines. It is worth mentioning here that the characteristics of the best fitting lines were computed using a least square regression. In Table 2 the slope S and the origin ordinate Y of these lines for the various investigated cases are summarized, as well as the associated L and λ values as deduced from (Eq. 6 and 7):

Table 1. Total water content, frozen density and freezing temperature of foods.

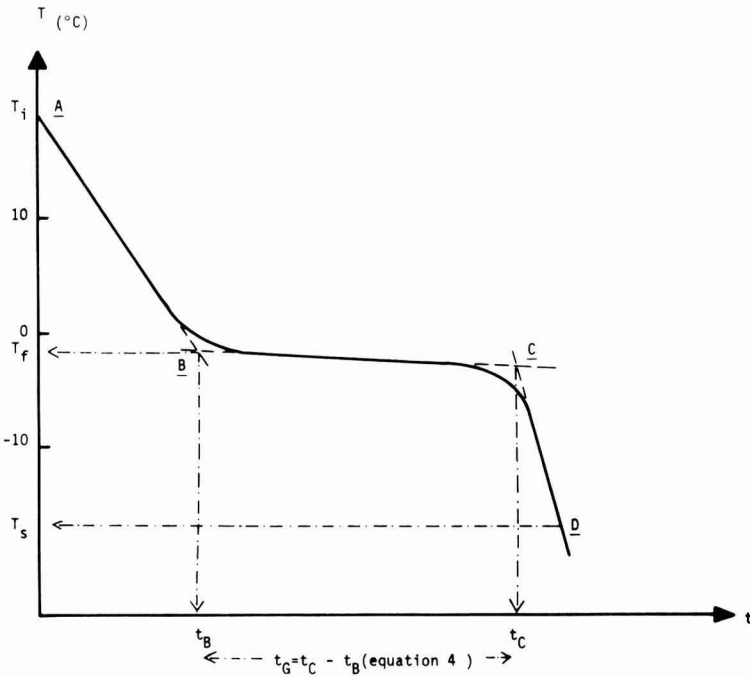| PRODUCT	TOTAL WATER CONTENT w (% product weight)	FROZEN DENSITY ρ (kg/m³)	INITIAL FREEZING TEMPERATURE T_f (°C)
Banana	73.5	1093	-2.3
Potato	80.0	990	-1.6
Carrot	88.0	954	-1.3
Turnip	94.0	897	-0.8
Cucumber	95.4	977	-0.5

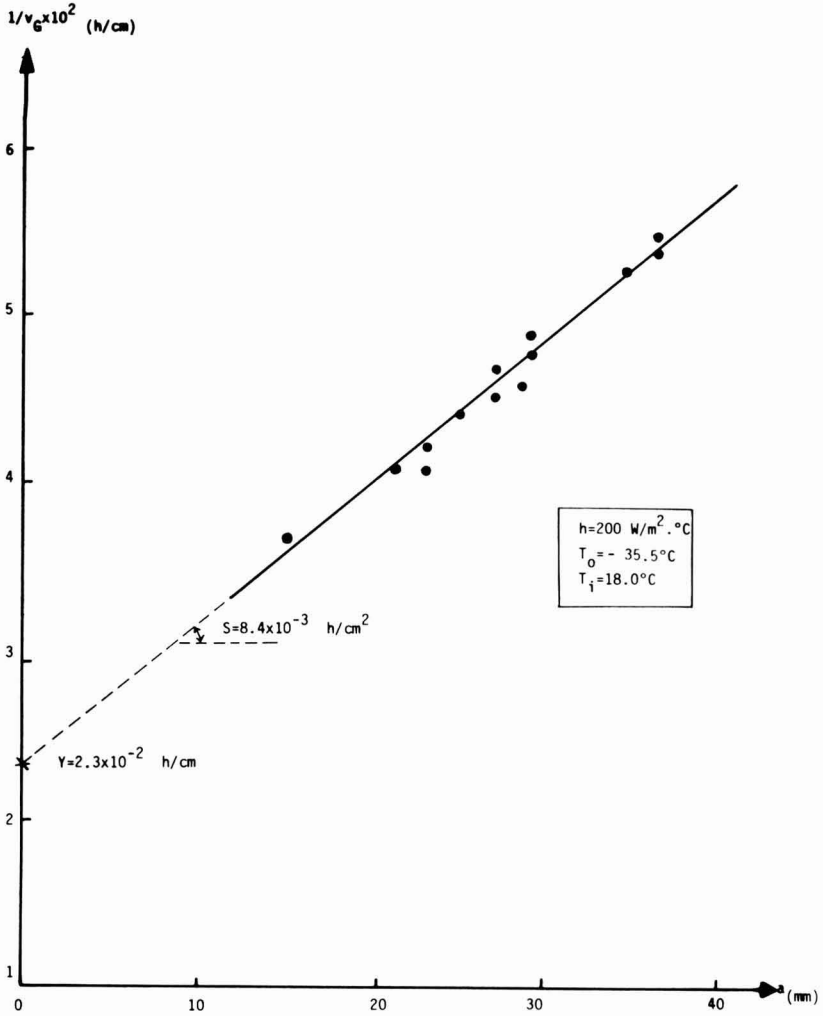FIG. 1. PRODUCT CORE TEMPERATURE EVOLUTIONS.

FIG. 2.   POTATO.

$$L = \frac{Y}{P} \cdot \frac{h}{\varrho} \cdot \frac{T_f - T_o}{2} \tag{6}$$

$$\lambda = \frac{Y}{S} \cdot \frac{R}{P} \cdot h \tag{7}$$

From them it appears clearly that the so-determined latent heats and thermal conductivities are all the larger as the total water content is higher.
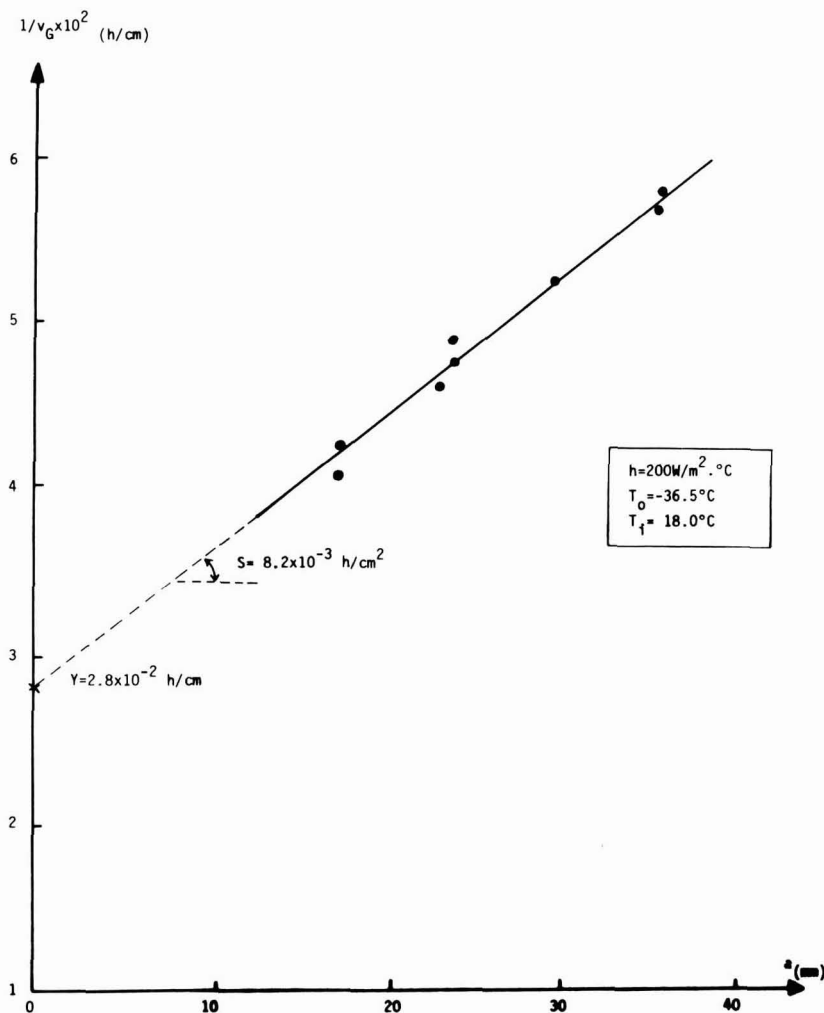
FIG. 3. CARROT.

DISCUSSION

Latent Heat

Literature (Heldman 1975) clearly indicates that the whole water kept in biological materials does not freeze immediately on reaching T_f. In fact crystallization progressively takes place between this upper value ordinarily close to $0\,°C$, and a lower limit generally about $-30\,°C$. However, it must be noted that most of the liquid phase turns into ice during the properly called freezing step, only the remainder of the fluid
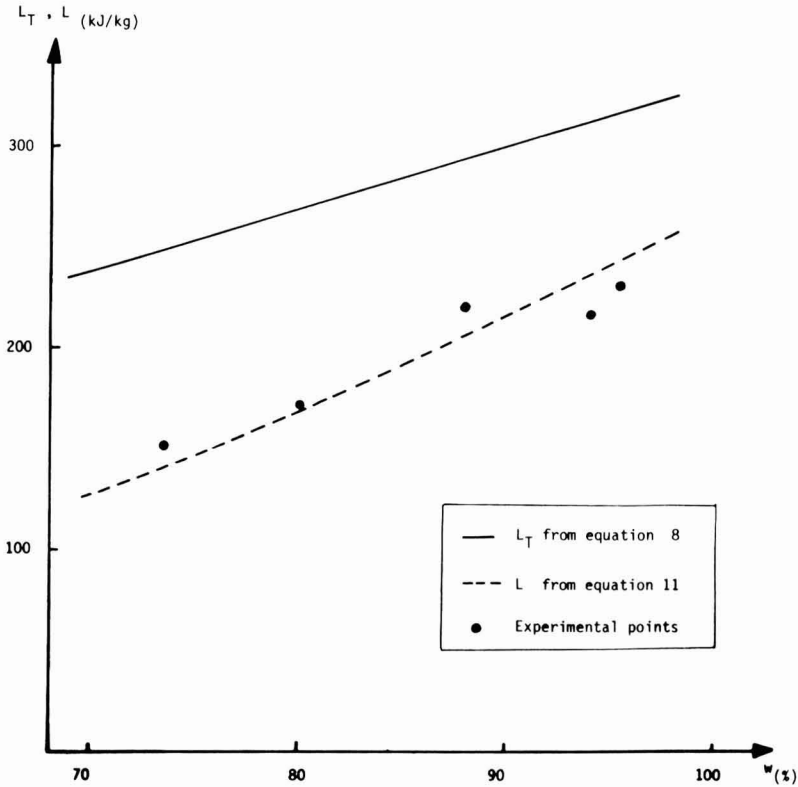
FIG. 4.   LATENT HEAT OF FOODS.

being frozen during the following refrigeration step. For conciseness in what follows the term L_T will be used to denote the heat that must be removed from a product to freeze the whole water kept in it. Generally it is admitted that (Eq. 8):

$$L_T = w \cdot \Lambda \tag{8}$$

where Λ represents the heat of fusion of ice (335 kJ/kg).

As it appears from Fig. 4 the L-values that have been determined in this study are lower than L_T. Making the assumption that there is a linear dependence between the latent heat removed from the product at freezing step, L, and the percentage of water actually frozen, f, well in accordance with the entire approach, a quick calculation of f-values may be performed with the help of equation (Eq. 9):

$$L = f \cdot L_T \tag{9}$$

The obtained values are reported in Table 2. On the whole they agree well with

Table 2. Estimated properties of foods.

PRODUCT	STRAIGHT LINE CHARACTERISTICS		LATENT HEAT L (kJ/kg)	FROZEN WATER PERCENTAGE f (%)	THERMAL CONDUCTIVITY λ (W/m^{o}C)
	$S \times 10^3$ (h/cm^2)	$Y \times 10^2$ (h/cm)			
Banana	9.7	2.2	152	62	1.11
Potato	8.4	2.3	173	65	1.39
Carrot	8.2	2.8	222	71	1.70
Turnip	6.2	2.4	218	71	1.94
Cucumber	7.1	2.9	233	72	2.06

literature data (Riedel 1951; Dickerson 1969), and may be roughly correlated through (Eq. 10):

$$f = 0.8 \, w \tag{10}$$

which suggests that the enthalpy change during the freezing step corresponds to the latent heat required to freeze 80% of the entrapped water.

Finally an equation fitting data points to better than $\pm 10\%$, and affording a direct estimation of L from the total water content w may be written (Eq. 11):

$$L = 268 \, w^2 \tag{11}$$

Obviously the latent heat values so predicted are in close touch with the Fluidized Bed Freezing process under consideration. Their use beyond these conditions, when the external heat exchange conditions are changed, must be strongly questioned.

Thermal Conductivity

In Fig. 5, experimental values of λ have been plotted as well as Lentz and Van Den Berg data curve for fruits and vegetables (1977). Data analysis reveals that there is a good agreement between them.

By simply making the assumption of the linear dependence of λ on λ_i, λ_d, λ_w the thermal conductivities of ice, dry matter and water (Eq. 12):

$$\lambda = (1 - w) \cdot \lambda_d + w \cdot [f \cdot \lambda_i + (1 - f) \cdot \lambda_w] \tag{12}$$

and using Eq. 10, a good fitting relation between λ and w has been found (Eq. 13):
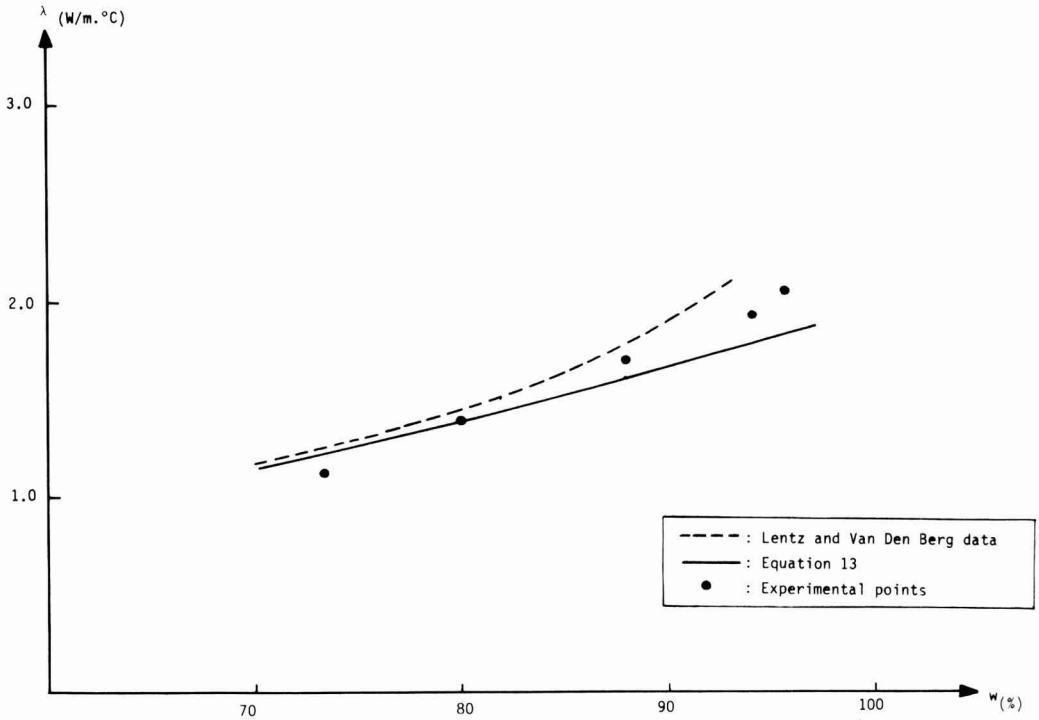
FIG. 5.　THERMAL CONDUCTIVITY OF FOODS.

$$\lambda = 1.36 \ w^2 + 0.34 \ w + 0.26 \tag{13}$$

The following values for water, ice and dry matter conductivities have been adopted: $\lambda_w = 0.6 \ W/m\,°C$; $\lambda_i = 2.3 \ W/m\,°C$; $\lambda_d = 0.26 \ W/m\,°C$ (Harper and El Sahrigi 1964; Perry and Chilton 1973).

CONCLUSION

The new method proposed to determine frozen food properties relates to Fluidized Bed Freezing of small food pieces immersed in a cold fluidized bed of fine particles, or even to other processes in which uniform and high heat transfer coefficients ($h \geqslant 200$ $W/m^2\,°C$) prevail at the product surface. It may be applied with confidence if (Eq. 14):

$$1 \leqslant Bi \leqslant 6 \tag{14}$$

$$\frac{T_o - T_f}{T_i - T_f} \leqslant 2 \tag{14a}$$

and works all the better as the total water content of materials is higher.

It starts from the fact that the values of freezing times as determined either from the length of the nearly horizontal central line observed on the temperature-time recordings at product core, or from the well-known Plank equation are quite similar. So it can be written with a good accuracy (Eq. 15):

$$\frac{t_g}{a/2} = \left(\frac{2\varrho L}{T_f - T_o}\right) \cdot \frac{R}{\lambda} \cdot a + \left(\frac{2\varrho L}{T_f - T_o} \cdot \frac{P}{h}\right) \tag{15}$$

By plotting the graphical time values t_G as a function of the product thickness a, straight lines may be drawn, and the latent heats removed to bring the products below the freezing point L, as well as the thermal conductivities of the frozen material in this final state λ, may be deduced. Moreover making the assumption that L-values linearly depend upon the percentage of frozen water f, f-values may be simply estimated.

The method has been tested on various fruits and vegetables with high total water contents ($70\% \leqslant w \leqslant 100\%$), taken at room temperature and plunged into a cooling medium at about $-40\,°C$. It has been checked at first that water crystallization is incomplete at freezing step, in good accordance with literature (Eq. 16):

$$f = 0.8\ w \tag{16}$$

Moreover it has been established that L and λ values may be estimated through (Eq. 17 and 18):

$$L = 268\ w^2 \qquad (\text{kJ/kg}) \tag{17}$$

$$\lambda = 1.36\ w^2 + 0.34\ w + 0.26 \qquad (W/m\,°C) \tag{18}$$

These relations are very useful for freezing time calculation in Fluidized Bed. But their use beyond the working conditions previously mentioned must be strongly questioned.

NOMENCLATURE

a = product thickness   m

Bi = Biot number ($Bi = \dfrac{h}{\lambda} \cdot \dfrac{a}{2}$)   —

f =	percentage of frozen water	—
h =	heat transfer coefficient	$W/m^2\,°C$
L =	latent heat corresponding to f	J/g
L_T =	latent heat corresponding to w	J/g
P,R =	dimensionless numbers	—
t_G =	graphical estimation of freezing time	s
t_p =	Plank estimation of freezing time	s
T_f =	initial freezing temperature	°C
T_i =	initial product temperature	°C
T_o =	outside cooling medium temperature	°C
T_s =	stocking temperature	°C
U_{mf} =	minimum fluidization velocity	m/s
v_G =	graphical estimation of mean freezing rate	m/s
w =	total water content (% product weight)	—
λ =	thermal conductivity of frozen food	$W/m\,°C$
λ_d =	dry matter thermal conductivity	$W/m\,°C$
λ_i =	ice thermal conductivity	$W/m\,°C$
λ_w =	water thermal conductivity	$W/m\,°C$
Λ =	latent heat of fusion of ice	J/g
ϱ =	frozen product density	kg/m^3

REFERENCES

CHARM, S. E. 1971. *The Fundamentals of Food Engineering* Avi Publishing Co., Westport, Conn.

DICKERSON, R. W., Jr. 1969. Thermal properties of foods In *The Freezing Preservation of Foods* Fourth Ed. Vol. 2 Avi Publishing Co., Westport, Conn.

FENNEMA, O. R., POWRIE, W. D. and MARTH, E. H. 1973. *Low Temperature Preservation of Foods and Living Matter* M. Dekker, London.

HARPER, J. C. and EL SAHRIGI, A. F. 1964 *Thermal Conductivities of Gas-Filled Porous Solids*-Ind. Engr. Chem. Fundamentals *3*, 318.

HELDMAN, D. R. 1975. *Food Process Engineering* Avi Publishing Co., Westport, Conn.

LENTZ, C. P. and VAN DEN BERG, L. 1977. Thermal conductivity data for foods: their significance and use. A.S.H.R.A.E. Journal 533.

MARIN, M. 1982. Freezing of foods in Fluidized Floatation Cell Engineering Doctor Thesis. Montpellier, France.

MARIN, M., RIOS, G. M. and GIBERT, H. 1983. Freezing of food products in a Fluidized Floatation Cell J. Powder and Bulk Solid Technol. 7, 1, 21.

PERRY, R. H. and CHILTON, C. H. 1973. *Chemical Engineers' Handbook* Fifth Ed. McGraw Hill-Kogakusha, New York and Tokyo.

RIEDEL, L. 1951 The refrigeration effect required to freeze fruits and vegetables. Refrig. Engr. *59*, 670.

QUANTITATIVE ANALYSIS OF TEXTURE CHANGE IN COD MUSCLE DURING FROZEN STORAGE

YOON J. KIM

Department of Food Science and Human Nutrition
Michigan State University
East Lansing, Michigan 48824-1224

DENNIS R. HELDMAN

Campbell Institute for Research and Technology
Campbell Place
Camden, New Jersey 08101

ABSTRACT

The textural deterioration of cod muscle during frozen storage was investigated by objective measurement using the Instron Universal Testing Machine. The rates of texture change as a function of storage time revealed that the increased toughness and decreased cohesiveness could be described by a first-order relationship. Higher storage temperatures resulted in more rapid rates of textural deterioration. Larger activation energy constants for toughness of cod muscle as compared to cohesiveness indicated that toughening was more temperature dependent than cohesiveness. The increased toughness and the decreased cohesiveness of frozen-stored fish appeared to be related to the protein denaturation of the cod muscle and the loss of water-holding capacity, respectively.

INTRODUCTION

The quality and shelf-life for various species of frozen fish during storage are measured organoleptically for either flavor or texture changes. The rate at which these changes occur varies with the handling and processing techniques employed prior to, during, and after freezing.

Freezing is recognized as one of the best methods of fish preservation. However, even at temperatures as low as $-20\,°C$, loss of tenderness and of water-holding capacity and characteristic fish flavor are the important changes associated with the freezing and low temperature storage of fish (Dyer 1951; Connell 1962). Prolonged storage brings about significant deterioration of the texture of frozen fish described as increased toughness, chewiness, rubberiness, or stringiness. After frozen storage, the

formation of drip after thawing causes undesirable characteristics of the cooked fish, which were then described as dry or lacking in succulence.

The mechanisms of texture change during frozen storage are not completely understood, but experimental evidence indicates that the development of toughness is associated with gradual denaturation of fish muscle protein (Love 1956; Dyer *et al.* 1957; Connell 1964; Hawthorne and Rolfe 1968). In some species, denaturation of muscle proteins measured by the loss of solubility appears to be closely related to the increased toughness observed by subjective and/or objective evaluation of texture (Dyer and Morton 1956; Connell 1962; Van Arsdel *et al.* 1969; Gill *et al.* 1979). According to Connell (1962), the denaturation of protein during frozen storage is also reflected as a drastic decrease of water-holding capacity; however, no relation has been reported between textural changes of cod muscle and loss of water-holding capacity of frozen-stored fish.

The objective of this study was to investigate the rate of textural deterioration of cod muscle as affected by frozen storage temperature. An attempt has also been made to relate textural changes of cod muscle to the changes in functional properties of the frozen-stored fish.

EXPERIMENTAL

Material

Commercially prepared unglazed fish portions (4 oz of $9.5 \times 7.0 \times 1.0$ cm) were obtained from Blue Water Seafoods, New Bedford, MA. The individual fish portions were packaged in aluminum pouches (4 mil thickness) to prevent dehydration and stored at $-7\,°C$, $-10\,°C$ and $-18\,°C$ for 60 days. Samples were removed at 15 day intervals, tempered at $0\,°C$, cut into cylindrical shapes ($D = 2.2$ cm) and then thawed ($0\,°C$) until the center of the sections reached $0\,°C$ prior to texture measurements.

Objective Evaluation of Texture

Texture profile analysis reported by Szczesniak *et al.* (1963) provides for measurement of specific parameters by both sensory and objective methods. Bourne (1968) adapted the texture profile method to the Instron Universal Testing Apparatus.

Objective texture measurements were conducted with an Instron Universal Testing Machine, Model TM, 50 kg capacity, with standard crosshead speeds of 0.05 to 50 cm/min. A flat probe ($D = 5.7$ cm) was attached to the crosshead and the stroke length was set to deform 20% of sample height twice in a reciprocating motion. The crosshead speed was 5 cm/min and a chart speed of 20 cm/min was used.

Three to four fish samples were used to evaluate the texture parameters at each time interval. The height of the force peak on the first compression cycle was defined as toughness. The ratio of the force areas under the first and second compressions (A_2/A_1) was defined as cohesiveness. The areas were measured by a planimeter. The

values of toughness and cohesiveness were obtained from 6 to 8 determinations of dark and white muscle sections of cod sample.

Analysis of Textural Deterioration with Storage Time

The loss of food quality as a function of storage time can be represented by a following mathematical equation (Eq. 1):

$$\frac{dC}{dt} = kC^n \tag{1}$$

where: C = quality factor measured
 t = time
 k = a rate constant
 n = the order of the reaction
 $\dfrac{dC}{dt}$ = the rate of change of C with time

In order to obtain the rate of textural deterioration, the texture parameters must be plotted versus time on logarithm coordinates. The rate constants and other kinetic parameters were estimated by the KINFIT Computer Program (Dye and Nicely 1971).

Effect of Storage Temperature

The influence of temperature on the rate constants (k) at which the texture is deteriorated during frozen storage was evaluated using the Arrhenius equation (Eq. 2)

$$k = A \exp\left[\frac{-Ea}{RT} \right] \tag{2}$$

where: A = Pre-exponential factor
 Ea = Activation energy constant
 R = Gas constant
 T = Absolute temperature in °K

The analysis leads to the evaluation of the activation energy constant (Ea).

RESULTS AND DISCUSSION

Typical force-deformation profile for cod muscle at time zero is illustrated in Fig. 1. The semi-logarithmic plots of toughness and cohesiveness versus storage time gave straight lines (Fig. 2 and 3), suggesting first-order kinetics. The value of toughness increased with time, whereas the cohesiveness parameter decreased during storage.
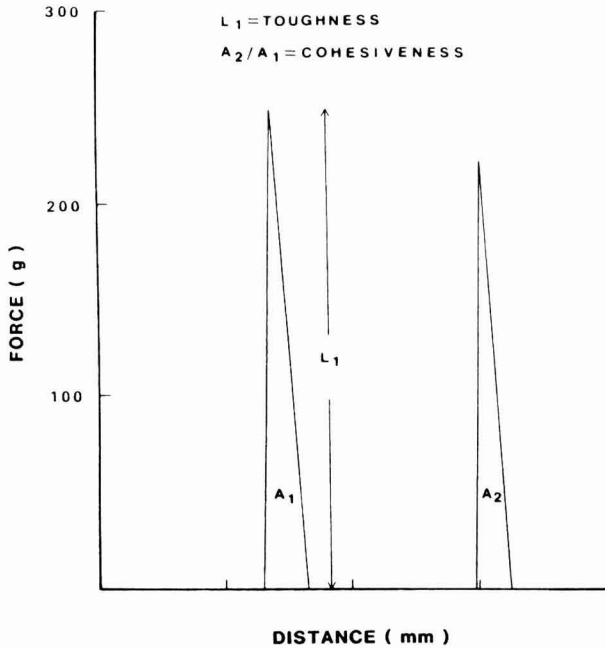
FIG. 1.   TYPICAL INSTRON FORCE-DEFORMATION TRACES OF COD MUSCLE SAMPLE
          AT TIME ZERO.

However, cohesiveness did not decrease as much proportionately as the increase of toughness and there was greater scatter in experimental points, resulting in a larger standard deviation (Tables 1 and 2). Cohesiveness is defined as the quotient: area A_2/area A_1. Small fluctuations at A_1 and A_2 may result in larger fluctuations in the cohesiveness value.

Connell (1964) and Hawthorne and Rolfe (1968) have done extensive research on the measurement of protein denaturation associated with the development of toughness in cod muscle during frozen storage. It is not yet fully known which myofibrillar proteins are particularly susceptible to the gradual denaturation due to the formation of various intermolecular covalent cross-links. The increased toughness measured by objective method with storage time, as the results shown in Table 1 and Fig. 2., indicated that protein denaturation found by other researchers contributed to the textural deterioration of cod muscle during frozen storage.

Corey (1970) defined the cohesiveness obtained from texture profile analysis as the strength of internal bonds making up the body of the products. Connell (1964) stated that the main reason for fish becoming tough and losing water-holding capacity is increased bonding between myofibrillar protein. Bonding resulted in cross-linking of fibrous protein network and at the same time coarsened the structure of bonds, consequently reducing its ability to hold water. As shown in Table 2 and Fig. 3, a very slow decrease in values of cohesiveness was due to the formation of various inter-

Table 1. First-order constants of toughness determined at various storage temperatures.

TEMPERATURE (°C)	RATE CONSTANT k (Day^{-1})	STANDARD DEVIATION
-7	0.1311×10^{-1}	0.717×10^{-3}
-10	0.1157×10^{-1}	0.754×10^{-3}
-18	0.8038×10^{-2}	0.990×10^{-3}

Table 2. First-order rate constants of cohesiveness determined at various storage temperatures.

TEMPERATURE (°C)	RATE CONSTANT k (Day^{-1})	STANDARD DEVIATION
-7	0.1730×10^{-2}	0.762×10^{-3}
-10	0.1511×10^{-2}	0.736×10^{-3}
-18	0.1402×10^{-2}	0.836×10^{-3}

Table 3. Activation energy (Ea) for toughness and cohesiveness of cod muscle.

TEXTURE PARAMETER	Ea (kJ/mole)	STANDARD DEVIATION
Toughness	25.4	0.16
Cohesiveness	10.0	5.25

molecular covalent cross-links of myofibrillar proteins, followed by a loosening of three-dimensional cross-linking structure of cod muscle. The decreased cohesiveness of cod muscle found in this study seems to be responsible for the loss of water-holding capacity of frozen-stored fish.

Since some fluctuation of storage temperature is occurring in commercial storage warehouses, it is useful to know the temperature dependence of quality loss during frozen storage. Thus, the Arrhenius equation is used to account for temperature dependence of the deterioration rate. Based on the rate constants (Tables 1 and 2) of texture parameters determined at various storage temperatures, an Arrhenius plot ($ln(k)$ vs $1/T$) was used to determine the activation energy constants. The results are given in Table 3.

As shown in Tables 1 and 2, the higher storage temperature resulted in faster rates of textural deterioration of cod muscle. Love (1962), Connell (1964) and Cowie
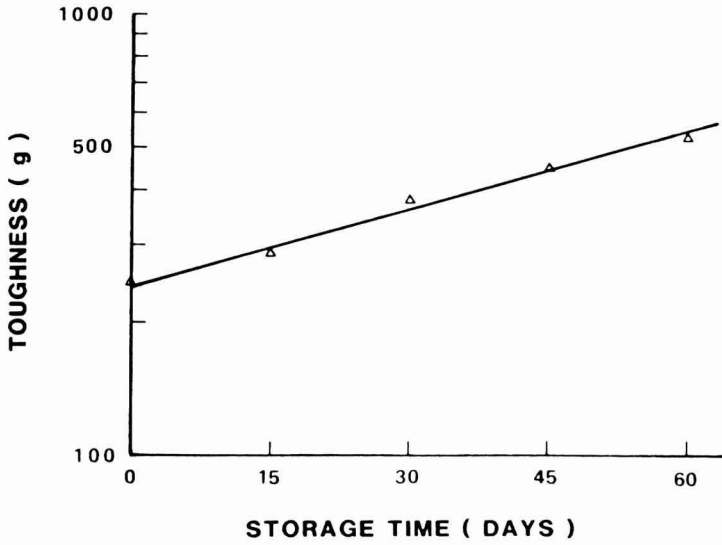
Y. J. KIM and D. R. HELDMAN

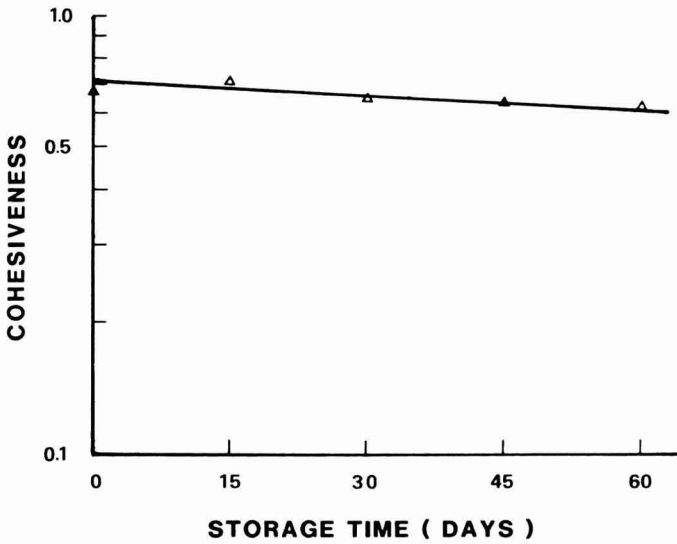FIG. 2.   A FIRST-ORDER PLOT FOR TOUGHNESS OF COD MUSCLE STORED AT −7C.

FIG. 3.   A FIRST-ORDER PLOT FOR COHESIVENESS OF COD MUSCLE STORED AT
          −7C.

and Little (1967) reported that the higher the temperature of frozen storage, the faster the rate of textural deterioration caused by protein denaturation. The results obtained in this study were in agreement with earlier reports. The activation energy constant (Table 3) for toughness was greater than that of cohesiveness, indicating that development of toughness was more influenced by temperature change than cohesiveness.

CONCLUSIONS

(1) The rate of textural deterioration of cod muscle during frozen storage can be described by a first-order relationship.
(2) The increased toughness of frozen fish with storage time results from protein denaturation of cod muscle, while the decreased cohesiveness results in the loss of water-holding capacity.
(3) The larger activation energy constant for toughness indicates more influence of temperature on rate constants for toughness as compared to rate constants for cohesiveness.

REFERENCES

BOURNE, M. C. 1968. Texture profile of ripening pears. J. Food Sci. *33*, 223.

CONNELL, J. J. 1962. Changes in amount of myosin extractable from cod flesh during storage at −14 °C. J. Sci. Food Agric. *13*, 607.

CONNELL, J. J. 1964. Fish muscle proteins and some effects on them of processing. In *Symposium on Foods: Proteins and Their Reactions*. (H. W. Schultz and A. F. Anglemier, Eds.), pp. 255, AVI Publishing Co., Westport, CT.

COREY, H. 1970. Texture in foodstuffs. Crit. Reviews in Food Sci. & Nutr. *1*, 161.

COWIE, W. P. and LITTLE, W. T. 1966. The relationship between toughness of cod stored at −29 °C and its muscle protein solubility and pH. J. Food Technol. *1*, 355.

DYE, J. L. and NICELY, V. A. 1971. A general purpose of curve fitting program for class and research use. J. Chem. Edu. *48*, 443.

DYER, W. J. 1951. Protein denaturation in frozen and stored fish. Food Res. *16*, 522.

DYER, W. J. and MORTON, M. L. 1956. Storage of frozen plaice and fillets. J. Food Res. Board of Can. *13*, 129.

DYER, W. J., FRASER, D. I. and MAC CALLUM, W. A. 1957. Further study of the influence of short storage periods, 3 days to 2 weeks at 15 °F, on the quality of frozen cod stored at 0 °F. J. Fish Res. Board Can. *14*, 925.

GILL, T. A., KEITH, R. A. and LALL, B. S. 1979. Textural deterioration of red hake and haddock muscle in frozen storage as related to chemical parameters and changes in the myofibrillar proteins. J. Food Sci. *44*, 661.

HAWTHORNE, J. and ROLFE, E. J. 1968. *Recent Advances in Food Science*, Vol. 4. Pergamon Press, Oxford, England.

LOVE, R. M. 1956. Influence of freezing rate on the denaturation of cold-stored fish. Nature. *178*, 988.

LOVE, R. M. 1962. Protein denaturation in frozen fish. VI. Cold storage studies on cod using the cell fragility method. J. Sci. Food Agric. *13*, 269.

SZCZESNIAK, A. A., BRANDT, M. A., and FRIEDMAN, H. 1963. Development of standard scales for mechanical parameters of texture and correlation between objective and sensory methods of texture evaluation. J. Food Sci. *28*, 397.

VAN ARSDEL, W. B., COPLEY, M. J. and OLSON, R. D. 1969. *Quality and Stability of Frozen Foods*. John Wiley & Sons, New York.

SIMULATION OF THAWING OF FOODS USING FINITE ELEMENT METHOD

H. ABDALLA and R. PAUL SINGH

Department of Agricultural Engineering
University of California, Davis, CA 95616

INTRODUCTION

Prediction of temperature distribution in foods, subjected to freezing or thawing, is an important topic in food processing. Such knowledge is useful in the design of equipment and the evaluation of storage and handling practices. There are many formulas available for estimating transient state heat conduction in a solid body which undergoes a phase change. The most used exact solutions to predict the freezing as well as the thawing times are Plank's equation and Newmann's solution (Bakal and Hayakawa 1973; Purwadaria 1980). These solutions are limited to the fact that they assume constant thermal properties throughout the freezing and thawing processes. In addition, they assume certain boundary conditions and treat only simple geometrical shapes.

Numerical solutions are obtained usually by applying either finite difference or finite element techniques. Since there are relatively few mathematical restrictions in solving equations by these techniques, they are used to obtain the solution for objects of complex geometrical shapes common to foodstuffs. Several researchers have utilized the finite difference procedure with temperature dependent physical properties to solve the freezing problem (Charm *et al.* 1973; Fleming 1973; Lescano 1973; Joshi and Tao 1974; Heldman and Gorby 1974b; Cleland and Earle 1977a; Hsieh *et al.* 1977). Comini and Bonacina (1974), DeBaerdemaeker *et al.* (1977), Singh and Segerlind (1974) and Naveh and Pflug (1983) implemented the finite element procedure for estimating the freezing time and heat conduction in foodstuffs. While the finite element analysis has proved useful in solving linear and nonlinear heat transfer problems, no investigation has been conducted to solve the thawing problem using the finite element procedure. All the previous investigations have assumed that the thawing problem is identical to the freezing problem and any solution valid for freezing should also hold for thawing. Most published models overlook the fact that during the thawing process, if the thawing environment involves condensation of water on the product, the rate of heat transfer can change dramatically.

The primary goal of this study was to develop a numerical model using the finite element method to predict the rate of freezing and thawing of food products.

THEORY

Governing Equations

Heat conduction is the primary mode of heat transfer in food freezing and thawing. The research reported in this paper considered heat conduction in an axisymmetric body. The governing differential equation is a Fourier type heat conduction problem (Carslaw and Jaeger 1959). The transient heat conduction for an axisymmetric shaped body with internal heat generation is as follows (Eq. 1):

$$\frac{1}{r}\frac{\partial}{\partial r}\left(rk_{rr}\frac{\partial T}{\partial r}\right) + \frac{\partial}{\partial z}\left(k_{zz}\frac{\partial T}{\partial z}\right) + \dot{q} = \varrho c_p \frac{\partial T}{\partial t} \tag{1}$$

with boundary conditions (Eq. 2 and 3):

$$\frac{\partial T}{\partial r}(0, z, t) = 0 \tag{2}$$

$$k_{rr}\frac{\partial T}{\partial r} + k_{zz}\frac{\partial T}{\partial z} + q + h(T-T_\infty) = 0 \tag{3}$$

and initial condition (Eq. 4):

$$T(r,z,0) = T_0 \tag{4}$$

An important aspect of food freezing and thawing which cannot be overlooked is the change of the product properties. Of particular significance is the change of phase of water during the freezing and thawing processes. The properties of a food product during freezing and thawing are temperature dependent since the apparent specific heat and the thermal conductivity are both functions of temperature in the freezing zone or below the initial freezing point of the product. Due to the latter, this heat transfer problem is a strong nonlinear problem. Since the finite element procedure can be extended to solve nonlinear problems through iterative algorithms with rapid convergence properties, it is useful in solving freezing and thawing problems. Another feature of the finite element method is its ability to accommodate complex shapes and sizes such as those encountered in food products.

Physical Properties

Heldman (1974) and Heldman and Gorby (1974a) developed a mathematical model for the prediction of thermal properties based on the freezing point depression. This model, used in this study, has been successfully used by several researchers to predict the thermal properties of food product during freezing (Purwadaria 1980).

Finite Element Formulations

Galerkin Method. By using the Galerkin method of weighted residuals, the solution of the original partial differential Eq. 1 can be recast as an integral problem (Baca *et al.* 1978). Fundamentally, the Galerkin method is based on the integral of the product of the residual error ϵ and some set of weighting function ω_j. The result is Eq. 5):

$$\chi = \iint_D \epsilon \, \omega_j \, drdz \tag{5}$$

where the residual ϵ is defined in terms of the specific differential operators and the approximating functions for the dependent variables. By imposing the orthogonality constraint $\chi = 0$, the Galerkin functional becomes an error distribution principle (Taghavi-Shivazi 1983) by which the residual ϵ is minimized over the domain D (Baca *et al.* 1978). The integral over the entire domain can be partitioned into subdomains (elements) and the temperature distribution within each element is assumed to be (Eq. 6):

$$T^{(e)} \, (r,z,t) = \sum_{i=1}^{4} \, N_i \, (r,z) \, T_i \, (t) = [N] \, \{T\} \, ^{(e)} \tag{6}$$

where $T_i \equiv$ discrete nodal temperature

Substituting Eq. 6 into Eq. 1 and applying Galerkin's criterion we may write (Eq. 7):

$$\iint_{D^{(e)}} \, N_i \left[\frac{\partial}{\partial r} \left(rK_{rr} \frac{\partial T^{(e)}}{\partial r} \right) + \frac{\partial}{\partial z} \left(rK_{zz} \frac{\partial T^{(e)}}{\partial z} \right) + r\dot{q} - r\varrho c_p \frac{\partial T^{(e)}}{\partial t} \right] drdz \, = 0 \tag{7}$$

Equation 7 expresses the desired averaging of the error or residual within the element boundaries, but it does not account for the influence of the boundary. We use integration by parts (Green-Gauss theorem) to introduce the influence of the natural boundary conditions. Equation 7 could be written in the form (Eq. 8):

$$- \iint_{D^{(e)}} \left[rK_{rr} \left[\frac{\partial N}{\partial r} \right] \{T\}^{(e)} \, \frac{\partial N_i}{\partial r} + rK_{zz} \left[\frac{\partial N}{\partial z} \right] \{T\}^{(e)} \, \frac{\partial N_i}{\partial z} \right] drdz$$

$$+ \iint_{D^{(e)}} \, r\varrho c_p \, N_i \, N_j \frac{\partial T^{(e)}}{\partial t} \, drdz \, - \iint_{D^{(e)}} r\dot{q} \, N_i \, drdz$$

$$- \int \, [rqN_i - rh \, N_j \, \{T\}^{(e)} \, N_i + rhT_\infty N_i] \, ds = 0 \tag{8}$$

or as in matrix form (Eq. 9):

$$[P] \left\{ \frac{\partial T}{\partial t} \right\} + [C] \{T\} + \{F\} = 0 \tag{9}$$

Since the governing equation is nonlinear, the integral equations will give a set of nonlinear ordinary differential equations. A Newton-Raphson formulation could be incorporated into the integral equations which yields an iterative solution algorithm. The time derivative

$$\frac{\partial T}{\partial t}$$

is approximated using the following relation (Eq. 10), (Baca *et al.* 1978):

$$\left(\frac{\partial T}{\partial t} \right)_{m+1} = \frac{\alpha}{\Delta t} (T_{m+1} - T_m) + (1 - \alpha) \dot{T}_m \tag{10}$$

The Computer Program. A computer program was developed using the finite element technique to solve the phase change in food freezing and thawing for axisymmetric heat transfer problems. The program was modified from the computer-aided simulation written by Herrmann (1983) to predict the temperature distribution in steady-state heat conduction problems. The modifications included the following: the transient case in food freezing and thawing where the classical Newton-Raphson iteration scheme was used; the convective boundary condition; lumped formulation of the heat capacity matrix instead of the traditional consistent formulation (Segerlind 1983); and the nonlinear function of physical properties versus temperature as developed by Heldman and Gorby (1974a).

EXPERIMENTAL

The Karlsruhe Test Substance, developed at the Federal Research Institute in Karlsruhe, West Germany, (Specht *et al.* 1981) was prepared in the laboratory and used as a substitute for foodstuffs in the thawing as well as the freezing experiments. An air conditioning unit (Aminco-aire, Model 4-5591) was used for the thawing experiments. An air-blast chamber was used to freeze samples.

In order to obtain heat transfer coefficients which could adequately describe the convective boundary condition in the freezer, a transient lumped parameter heat transfer case with temperature independent thermal properties and without change of phase was selected. A copper sphere of 1 in. diameter located in the same place in the freezer

as the sample was assumed to provide acceptable geometric similitude. The heat transfer coefficient at each particular velocity of freezing medium was estimated.

Thermal conductivity, heat capacity and initial freezing point of Karlsruhe test substance were obtained from the literature (Specht *et al.* 1981). Density of the product was determined by weighing the product. The volume of the product was determined by the amount of displaced volume of water in a graduated cylinder. Thus density was established by dividing the weight by the volume (Table 1).

Table 1. Physical properties of Karlsruhe test substance.

Thermal Conductivity[a] kJ/m hr°K	Specific Heat[a] kJ/kg°K	Density[b] kg/m³	Initial Freezing Point[a] °C
3.4	3.8	1040	−0.7

[a]Values from literature.
[b]Values determined experimentally.

To test the mathematical model, a series of experimental trials were conducted. Thawing medium temperatures of 20 and 40°C were studied for two mean air velocities of 3.68 m/s and 1.18 m/s. The thawing medium relative humidity ranged from 25% to 85%. The experimental trials, selected on the basis of available apparatus, are shown in Table 2.

RESULTS AND DISCUSSION

Table 3 shows the results of the analytical solution of a one-dimensional heat conduction problem with constant thermal properties compared to the numerical solution using the finite element program at the same cross-section. The results show excellent agreement between the finite element solution and the analytical solution with errors ranging from a maximum of 1.75% at 5 and consistently decreasing to 0.24% at 40. The average error is 0.725%.

The results from finite element prediction model for freezing were compared with experimental data and results from the finite difference analysis used by Lescano (1973) to describe the freezing of rectangular slab-shaped codfish fillets. Figure 1 shows the predicted temperature history using the finite element method compared to the experimental results. The figure shows that the finite element prediction gave better agreement with the experimental results.

Figure 2 shows the results of simulation of the freezing process using the finite element method for the temperature history at the center of a sphere (diameter = 2.54

Table 2. Experimental trials for thawing of Karlsruhe test substance.

Experimental Variable	Trial Number											
	1	2	3	4	5	6	7	8	9	10	11	12
A	40	20	40	20	40	20	40	20	40	20	40	20
B	85	85	55	60	25	45	85	85	55	60	25	45
C	1.18	1.18	1.18	1.18	1.18	1.18	3.68	3.68	3.68	3.68	3.68	3.68
D	259	150	172.5	107	100	92.5	646	489	417	343	210	256

A = Thawing medium temperature, °C
B = Thawing medium relative humidity, %
C = Mean air velocity, m/s
D = Predicted mean convective heat transfer coefficient, $W/m^2 °C$

Table 3. Comparison of analytical and finite element solutions at $x=10$ cm
          Boundary condition: $T=50°$ C at $x=0$, $T=0°$ C at $x=\infty$;
          Intitial condition: $T=0°$ C at $t_3=0$; $k=4$ kJ/m²hr K; $\varrho C_p=1$ kJ/m³K.

Time (hr)	Analytical Solution (°C)	Finite Element Solution (°C)	Absolute Error	% error
5	5.69	5.79	0.10	1.75
10	13.18	13.01	0.17	1.28
15	18.07	17.90	0.17	0.94
20	21.46	21.33	0.13	0.60
25	23.97	23.87	0.10	0.40
30	25.93	25.84	0.09	0.30
35	27.51	27.43	0.08	0.29
40	28.81	28.74	0.07	0.24
		Average error	0.11	0.725

cm) of Karlsruhe test substance. These predictions were compared to experimental data from three replications at a heat transfer coefficient of 70 $W/m²°C$.

There is close agreement between the experimental and predicted results. Small discrepancies could be attributed to the location of the thermocouple, used to measure the temperature, not exactly at the geometric center of the sphere; fluctuations of the freezing environment temperature; the inherent measurement error of thermocouple; and the statistical errors in evaluating the heat transfer coefficient.

Using the different experimental conditions given previously in Table 2, thawing curves were determined experimentally for the Karlsruhe test substance. The results for a thawing temperature of 40 °C is shown in Fig. 3. The results represent duplicate trials. Four different relative humidities were selected for each temperature. The relative humidity of the air ranged from 25% to 85%. The selection of the humidities was limited by the available equipment.

Using a curve fitting procedure (Abdalla 1984), the effective convective heat transfer coefficients for the experimental thawing curves were predicted using the finite element model. It is obvious that during the thawing process, due to condensation, the convective heat transfer coefficient changes in magnitude. In this study an "effective" convective heat transfer coefficient is used which is a single value of the coefficient used for the entire temperature range.

The higher the humidity of the air the higher the heat transfer coefficient and vice
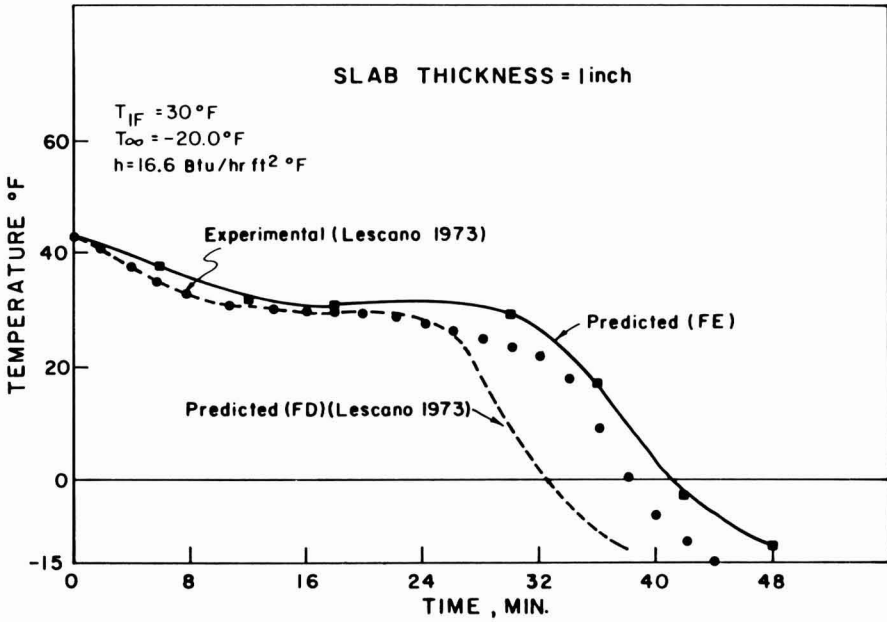
FIG. 1.   COMPARISON OF FINITE ELEMENT (FE) PREDICTION WITH EXPERIMENTAL
AND FINITE DIFFERENCE (FE) PREDICTION OF FREEZING OF 1 in.-THICK
FINITE SLAB OF CODFISH.
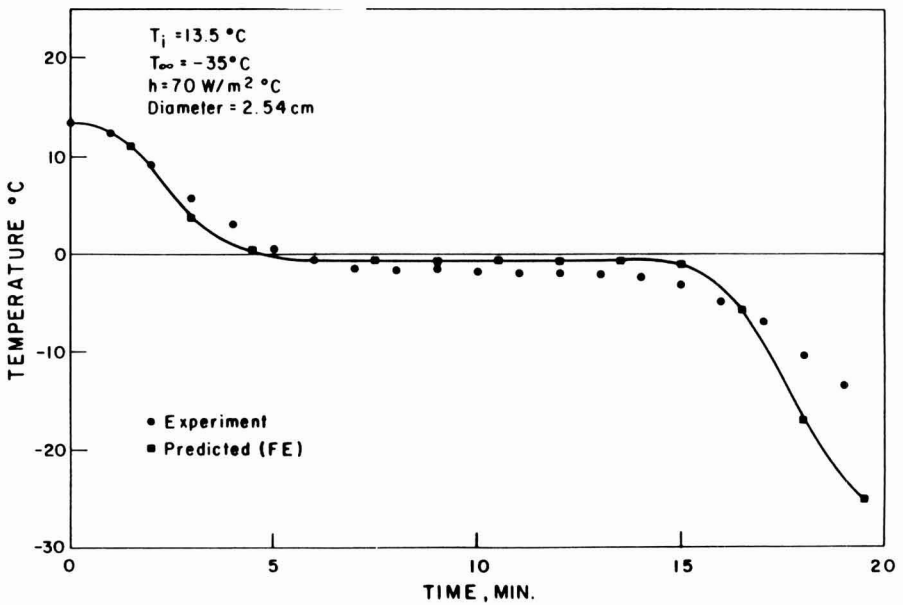
FIG. 2.   COMPARISON OF FINITE ELEMENT PREDICTION WITH EXPERIMENTAL
FREEZING CURVE OF A 2.54 cm KARLSRUHE TEST SUBSTANCE SPHERE.
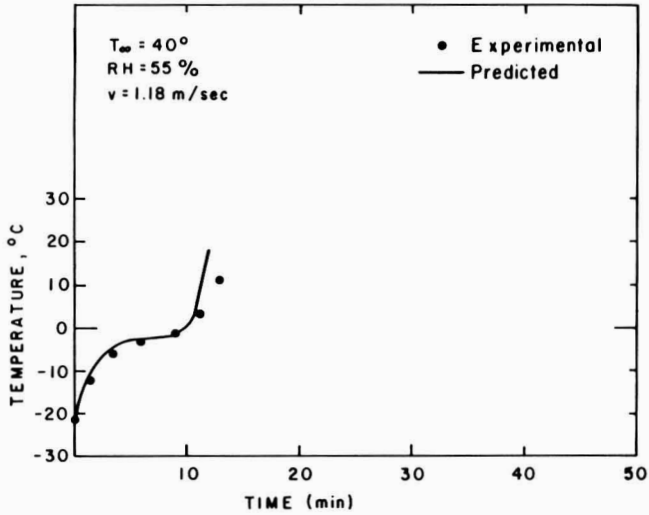
FIG. 3.   TEMPERATURE HISTORY AT THE GEOMETRIC CENTER OF A 2.54 cm
KARLSRUHE TEST SUBSTANCE SPHERE DURING THAWING.
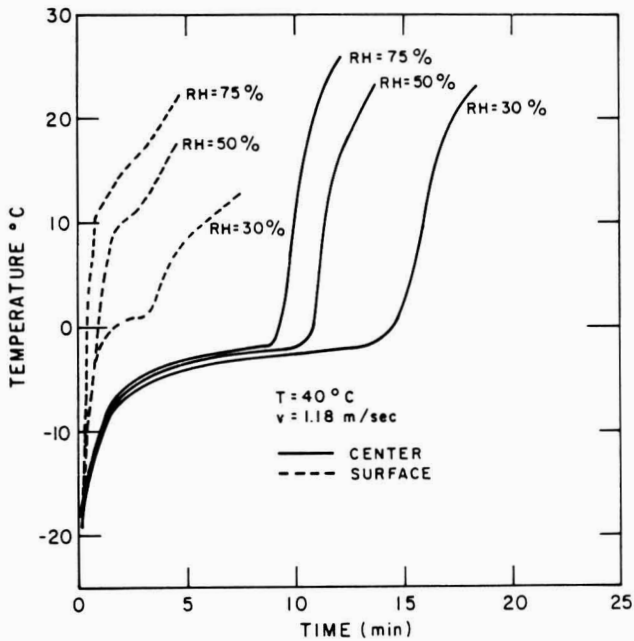
FIG. 4.   PREDICTED THAWING CURVES OF A 2.54 cm DIAMETER SPHERE OF
KARLSRUHE TEST SUBSTANCE AT DIFFERENT RELATIVE HUMIDITIES
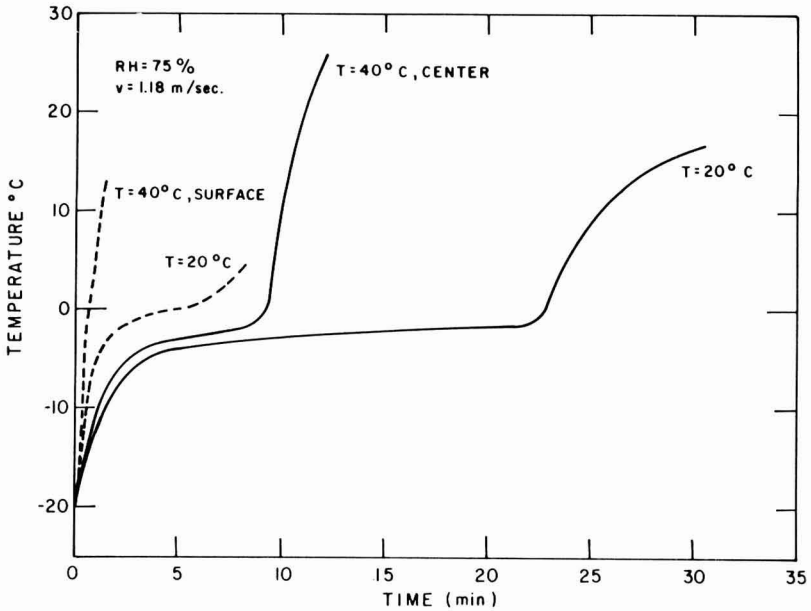
FIG. 5.   PREDICTED THAWING CURVES OF A 2.54 cm DIAMETER SPHERE OF
KARLSRUHE TEST SUBSTANCE AT DIFFERENT TEMPERATURES.

versa, since condensation plays an important role in enhancing the rate of heat transfer. On the other hand the higher the air velocity the higher the heat transfer coefficient since increasing the air velocity will increase the Reynolds number and hence Nusselt Number which is proportional to the heat transfer coefficient.

Temperature history curves were predicted for different thawing conditions. Three different relative humidities, namely 30%, 50% and 75% were selected. Figure 4 shows the results of these predictions. As expected, increasing the relative humidity of the air will increase the heat transfer coefficient and reduce the thawing time.

Figure 5 shows that the thawing environment temperature has a considerable influence on the heat transfer coefficient and hence on the rate of the thawing process. Increasing the air velocity will also increase the rate of the thawing process. Increasing the air velocity will also increase the rate of heat transfer. This is illustrated in Fig. 6. Figure 7 shows how the thawing front moves into the product with time. The rate at which the thawing front is moving slows down if the thawing temperature is lower.
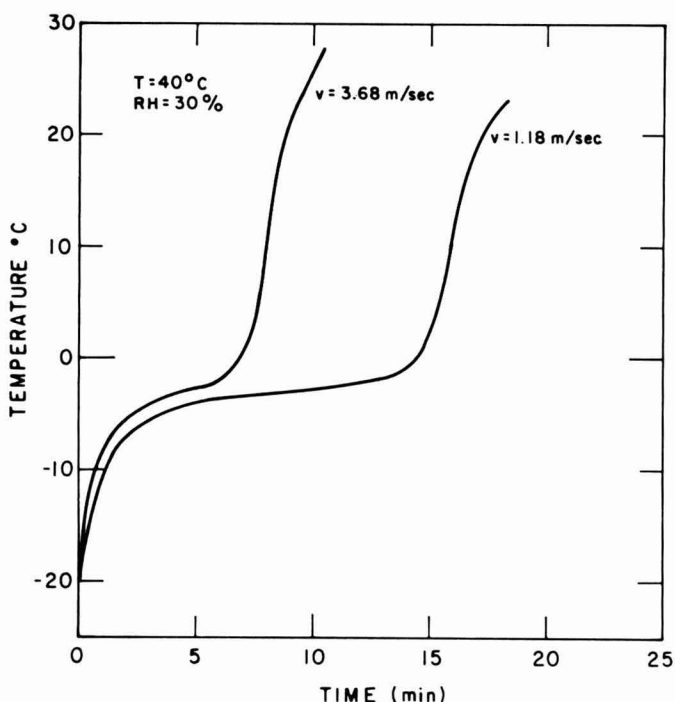
FIG. 6. PREDICTED TEMPERATURE HISTORIES AT GEOMETRIC CENTER OF A 2.54 cm
DIAMETER SPHERE OF KARLSRUHE TEST SUBSTANCE AT DIFFERENT AIR
VELOCITIES.

CONCLUSIONS

(1) A computer simulation using the finite element method was developed to
simulate freezing and thawing.

(2) Accuracy of the model was demonstrated when the predicted solution for a
one dimensional heat conduction with constant physical properties provided accept-
able agreement with the analytical solution. Also experimental freezing curves from
the literature were in satisfactory agreement with predicted values.

(3) The computer simulation was verified for freezing by experimental data from
freezing a 2.54 cm diameter sphere made of a model system (Karlsruhe test
substance).

(4) The computer program has the ability to accommodate various boundary con-
ditions as well as nonlinearity of product thermal properties during freezing and
thawing.
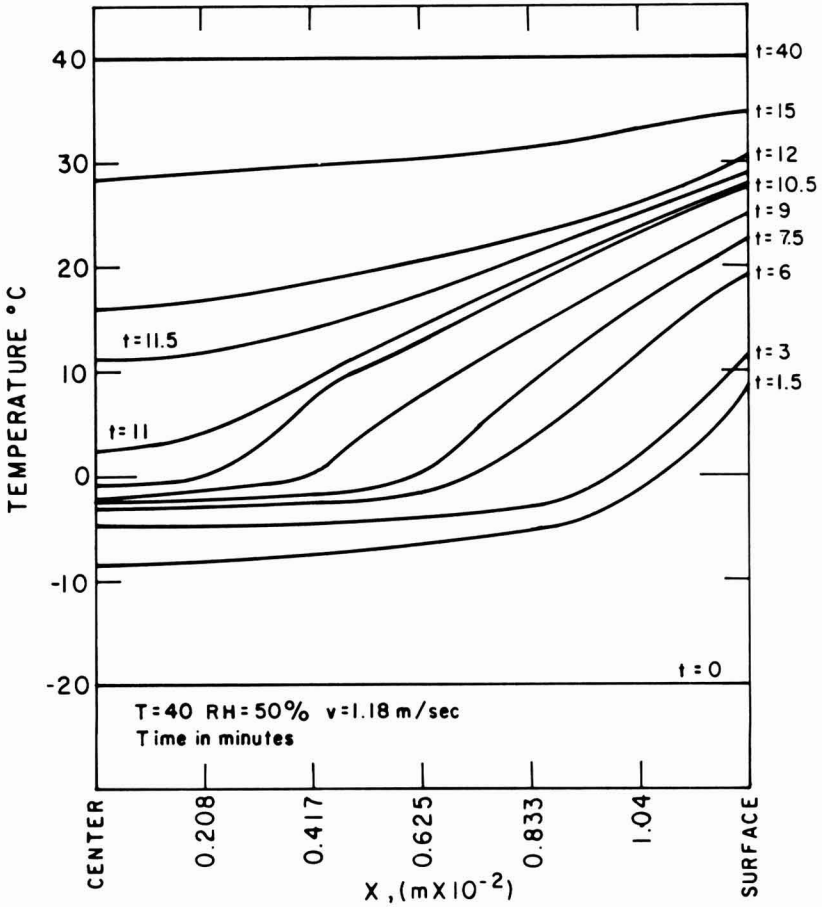
FIG. 7.   PREDICTED THAWING RATES ACROSS A 2.54 cm DIAMETER SPHERE OF
KARLSRUHE TEST SUBSTANCE.

LIST OF SYMBOLS

$[C]$ = Stiffness matrix defined in equation (9)
c_p = Specific heat of product, J/kg K
$\{F\}$ = Load matrix defined in equation (9)
h = Convective heat transfer coefficient, W/m²K
k = Thermal conductivity of product, W/m K
N = Shape function defined in equation (6)

$[P]$ = Capacitance matrix defined in equation (9)
q = Heat generation inside the body
RH = Relative humidity, %
r,z = Coordinates of quadrilateral nodes for axisymmetric element, m
s = Surface area, m^2
T = Temperature, °C
T_0 = Initial product temperature, °C
T_∞ = Ambient temperature, °C
$\dot{T}$ = Time derivative of temperature
t = Time, sec
ω = Weighting function defined in equation (5)
ϱ = Density, kg/m^3
α = Order of approximation defined in equation (10)
ϵ = Residual defined in equation (5)

Superscripts

$\cdot$ = First derivative with respect to time
m = Time level in finite difference scheme
e = A quadrilaterial finite element

REFERENCES

ABDALLA, H. O. 1984. Simulation of freezing and thawing in foods using the finite element method. Ph.D. thesis. Department of Agricultural Engineering, University of California, Davis.

BACA, R. G., KING, I. P. and NORTON, W. R. 1978. Finite element models for simultaneous heat and moisture transport in unsaturated soils. In *Finite Elements in Water Resources.* Pentech Press, London.

BAKAL, A. and HAYAKAWA, K. 1973. Heat transfer during freezing and thawing of foods. Advances in Food Res. *20*, 217.

CARSLAW, H. S. and JAEGER, J. C. 1959. *Conduction of Heat in Solids.* Claredon Press, Oxford, England.

CHARM, S. E., BRAND, D. H. and BAKER, D. W. 1972. A simple method for estimating freezing and thawing times of cylinders and slabs. ASHRAE J. *14* (11), 39.

CLELAND, A. C. and EARLE, R. L. 1977a. A comparison of analytical and numerical methods of predicting the freezing times of foods. J. Food Sci. *42*, 1390.

CLELAND, A. C. and EARLE, R. L. 1977b. The third kind of boundary condition in numerical freezing calculations. Int. J. Heat and Mass Transfer, 20, 1029.

COMINI, G. and BONACINA, C. 1974. Application of computer codes to phase-change problems in food engineering. Int. Institute of Refr. Meeting of Commissions B1, C1 and C2, Bressanone, Italy. Bulletin, Annexe, 15.

DE BAERDEMAEKER, J., SINGH, R. P. and SEGERLIND, L. J. 1977. Modelling heat transfer in foods using the finite element method. J. Food Proc. Eng., *1*, 37.

FLEMING, A. K. 1973. The numerical calculation of freezing processes. Proceedings of the XIII Int. Congress of Refr., *2*, 303.

GUTSCHMIDT, J. 1960. Uber Das Herstellung Und Verpacken Der Karlsruher Prufmasse. Kaltetechnik, 12 (8), 226-229.

HELDMAN, D. R. 1974a. Predicting the relationship between unfrozen water fraction and temperature during food freezing using freezing point depression. Trans. ASAE, *27*, 63.

HELDMAN, D. R. and GORBY, D. P. 1974a. Predictions of thermal conductivity in frozen food. ASAE Paper No. 74-6017.

HELDMAN, D. R. 1974. Predicting the relationship between unfrozen water fraction and temperature during food freezing using freezing point depression. Trans. Bressanone, Italy. Bulletin Annexe, 29.

HELDMAN, D. R. and SINGH, R. P. 1981. *Food Process Engineering*, 2nd Ed. AVI Publishing Co., Westport, CT.

HERRMANN, L. R. 1983. Personal Communications.

HSIEH, R. C., LEREW, L. E. and HELDMAN, D. R. 1977. Prediction of freezing times for foods as influenced by product properties. J. Food Proc. Eng. *1*, 183.

JOSHI, C. and TAO, L. C. 1974. A numerical method of simulating the axisymmetrical freezing of food systems. J. Food Sci. *39*, 623.

LESCANO, C. E. 1973. Predicting freezing curves in codfish fillets using the ideal binary solution assumption. M.S. Thesis. Department of Agricultural Engineering, Michigan State University, East Lansing, MI.

NAVEH, D. and PFLUG, I. J. 1983. The finite-element method in thermal processing of foods. J. Food Sci. 48(4), 1086-1093.

PURWADARIA, H. K. 1980. A Numerical Prediction Model for Food Freezing Using Finite Element Methods. Ph.D. Thesis. Department of Agricultural Engineering, Michigan State University.

SEGERLIND, L. J. 1976. *Applied Finite Element Analysis*. John Wiley and Sons, New York, N.Y.

SEGERLIND, L. J. 1983. Personal communications.

SINGH, R. P. and SEGERLIND, L. J. 1974. The finite element method in food engineering. ASAE Paper No. 74-6015.

SPECHT, H., KARIUS, H. and KUNIS, J. 1981. Zur Herstellung and Untersuchung von Gefrierprufmassen. Lebensmittelindustrie, 28, 12-13.

TAGHAVI-SHIRAZI SAYED-ALIEREZA. 1983. A Galerkin finite element model of infiltration into unsaturated porous media. M.S. Thesis, Civil Engineering Department, University of California, Davis.

WALPOLE, R. E. and MYERS, R. H. 1972. *Probability and Statistics for Engineers and Scientists*. MacMillan Publishing Co., New York.

PARTICLE SIZE CHARACTERIZATION OF SELECTED GRAINS UNDER WET GRINDING

E. U. U. ITUEN, J. P. MITTAL[1], and J. S. ADEOTI

Department of Agricultural Engineering, PMB 1044
Ahmadu Bello University, Zaria (Nigeria)

ABSTRACT

The particle size analysis of maize, sorghum and millet under wet grinding conditions was studied with a burr grinding mill (the type commonly used in the locality). Some constants regarding particle size and size distribution of the wet ground products such as the distribution modulus, the size modulus, and the geometric mean diameter were determined.

The ground material was wet seived in BS410 sieves with the aid of a dispersing agent, Calgon, which improved sieving, especially in the lower sieves.

The results of the dried sieve fractions were plotted as cumulative percent by weight versus particle diameter on a log-probability paper for the study of the particle size and size distribution characteristics. The geometric mean diameter (average particle size) of the ground product was observed to decrease with increase in moisture content, except that for maize which showed an initial rise before decrease. The size modulus, too, decreased with increase in moisture content but maize showed the usual deviation at the start of soaking in water. The distribution modulus in maize and sorghum was seen to decrease with increase in moisture content but that of millet increased slightly.

INTRODUCTION

A primary particle is described as one whose size can be further reduced only by forceful shearing of its crystalline or molecular bonds. It may consist of meshing crystallites in a crystalline material or a homogeneous mass of molecules in an amorphous material. It may also be represented as a cluster of particles. The particles are called flocs if they are only loosely attached to each other (as by Vander Waals forces) or agglomerates if they are strongly bonded at the point of contact (as by chemical bonds). A particulate material (powder) consists of a collection of flocs or agglomerates, or both.

Particle size analysis is the characterization of a particulate material to determine the various amounts of different separates in a sample. The characterization may

[1] Present address: M/S Bankey Lalom Prakash, Bisavli (Gadaun) VP 202520 India.

involve particle size measurement, particle shape and size distribution representations.

In the agricultural processing industry, grains and forages meant for human and animal consumption are reduced to smaller sizes (and perhaps after some processes) for eventual use. Particle size and size distribution are important in unit operations such as mixing, separation, extrusion and pneumatic handling of the powdered material.

Grinding may be dry or wet depending on choice or application of the end products. In Nigeria, wet and dry grindings are performed for making of such recipe as 'tuwo' from dry flour and 'ogi' from wet products. Characterization of dry and wet grain materials is, therefore, important in the design of grinding processes and equipment.

Most works on particle size analysis are under dry grinding conditions. However, particle size of rocks and stones has been characterized under wet grinding conditions (Fuerstenau and Sullivan 1961). Biological materials like cereal grains pose some problems during wet grinding because the particles swell as they come in contact with water and so cannot pass through the sieve aperture easily during sieving.

This study was undertaken to determine the size distribution parameters such as distribution modulus, size modulus and geometric mean diameter of cereal grains under wet grinding conditions.

THEORETICAL CONSIDERATIONS

Various methods have been used to represent characteristics of particle size distribution. A single parameter representation such as the mean particle size, and/or surface area of particle is generally inadequate to completely describe a distribution function. Hansen and Stewart (1965) indicated that using finest modulus alone to describe particle size is misleading since it represents only a small portion of the size distribution. They also stated that uniformity index which gives an additional information concerning distribution of sizes into coarse, medium and fine grades is also not adequate. Chung et al. (1977) indicated that particulate materials require at least two parameters to adequately describe their distribution function.

A number of equations to relate the distribution of a powdered material with particle size had been proposed by many researchers (Perry and Chilton 1973). Many researchers have used the Schumann's equation (Hansen and Stewart 1965) (given below) to a great success in characterizing the distribution of particles in size reduced agricultural materials (Eq. 1):

$$y = 100 \ \frac{(x)^{\alpha}}{(k)} \tag{1}$$

where x = particle size based on smallest sieve opening it will pass through.

y = weight (percent) finer than size x

k = product size modulus (representative sieve size which 100% of the product will theoretically pass through) largest particle size

α = distribution modulus.

A log-normal plot of this equation yields a straight line of slope which intersects the 100 percent ordinate line at a particle size k. The distribution modulus is constant for a product for different screen sizes. That is, the product passed through different screens have identical slope. The distribution modulus gives information on a range of sizes in the product. It represents products uniformity and is directly proportional in magnitude to the degree of uniformity (Hansen and Henderson 1972). The size modulus, k, indicated the approximate size of the largest particles of a significant quantity in a product.

A log-probability plot is now recognized by the American Society of Agricultural Engineers as the standard for reporting the fineness distribution of ground product (Henderson and Perry 1976). Log-probability particle size distribution can be described completely by two values, the geometric mean diameter, (dgw), and the geometric standard deviation, (sgw) which can either be calculated analytically with the help of the following expressions or can be obtained directly from a log-probability plot (Henderson and Perry 1976; ASAE Year Book 1979) (Eq. 2 and 3):

$$dgw = d50 = \text{particle diameter at 50\% probability} \qquad (2)$$

$$sgw = \frac{d84}{d50} = \frac{d50}{d16} = \frac{\text{Particle size at 84\% probability}}{\text{Particle size at 50\% probability}}$$

$$= \frac{\text{Particle size at 50\% probability}}{\text{Particle size at 16\% probability}} \qquad (3)$$

Headley and Pfost (1968) stated that since no distribution had ever been truly normal or log-normally distributed, some biological materials only closely approach log-normal distribution. The end of a straight line plot can be extrapolated to find parameters of the subsieve regions (Hansen and Stewart 1965).

MATERIALS AND METHODS

Selection of Materials

Maize, sorghum and millet grains were selected because of their popularity in the Nigerian diets and also because of current research interests. Maize grains were obtained from the National Seed Service whereas sorghum and millet grains were obtained from the Institute for Agricultural Research, both of Samaru, Zaria.

Grinding Operation

No. 1A Premier burr mill powered by a 5 kW lister diesel engine was used for grinding the grains. The Premier burr mill was used because of its popularity in the locality.

Initially, 1 kg of each cereal was ground dry. The same quantity of each cereal was then soaked in water for a definite time to acquire a certain moisture level. The time of soaking ranged from two hours to several hours or days. At the end of soaking, the grains were removed from water, tied in a piece of mosquito netting and the free water from it was drained off. The soaked grains were weighed again to determine the amount of moisture absorbed in that interval of time.

The grain was then ground at constant clearance of the mill. The feeding of the grains into the mill plates was also kept constant. The grinding was performed in one cycle. The grinding time and temperature were recorded. The moisture content was also determined from a sample of the ground product immediately after the grinding by the oven-dry method. The grinding experiment was performed in series, one cereal grain after the other.

Particle Size Analysis

The British Standard sieves BS 410 which consisted of sieve numbers 7, 14, 25, 52, 100 and 200 were used for sieving. The limit of sieving was kept at mesh 200 because this is the lowest sieve recommended by the American Society of Agricultural Engineers (ASAE) for effective sieving of cereal products (Hansen and Henderson 1972).

The sieves were first weighed empty. A sample of 100 g from the dry ground product was sieved for about 10 min on a Ro-tap machine. Sieving was interrupted after 5 min to remove any blockage of the sieve apertures. At the end of sieving, the sieves with sieved fractions were weighed and difference between them and their empty weights gave the weight of the fractions retained on the sieves.

In the wet sieving, 150 g of the wet ground sample was used (the increase in weight was due to the weight of moisture in it). The sample was dissolved in a container and 25 ml of 5% solution of a dispersing agent, Calgon, (sodium hexametaphosphate + sodium carbonate) was added and mixed well. The suspension was stirred for about 2 min and was then poured into the top sieve. The first sieve was removed and rinsed thoroughly with vertical movement in a basin of water. The water in the basin was then poured into the next sieve which was placed in the stack of sieves. The process continued with one sieve washed into another till the last. The sieve fractions were carefully washed out into well labeled small cans of known weights and dried in the oven.

RESULTS AND DISCUSSION

Grinding of Maize, Sorghum and Mill

It was observed that it was more difficult to grind millet than the other two grains, especially when it was soaked for 18 h and above. The grains could not flow easily into the mill. The ground material became pasty and much attrition heat was developed. Table 1 shows the effect of moisture content on the temperature of ground grains. Jindal (1975) also showed that increase in moisture content raised the temperature of ground corn in a hammer mill.

The grains took longer time for grinding as the moisture content increased. Thus the grinding capacity of these cereal grains decreased with increase in moisture content. Figure 1 shows the grinding capacity of various grains as affected by change in moisture content.

Maize soaked for two h produced very rough and big particles. This behavior of maize may be supported by the work of Brekke (1968) which showed that during tempering process (soaking in water) of corn, the highest rate of stress crack formation usually occurs between 0.5 and 2 h at temperatures ranging from 18.3 and 29.4 °C. It is believed that this highest stress crack formation resulted in a very rough grinding exhibited during the grinding by a sample soaked for 2 h. Rend (1962) suggested that starch gel in rice is brittle below 15% moisture content but plastic at higher moisture levels. It is supposed that the transition period between brittle stage at low moisture content and plastic stage at high moisture content for maize might have given a condition resulting in big particles during grinding. This transition period might have fallen between 0.5 and 2 h of soaking in water.

Wet Sieving

Wet sieving was easy with coarse grinding such as with maize soaked for 2 h. With fine grinding, the sieve fractions could not pass through the sieves of 52, 100 and 200 mesh easily. A dispersing agent was then added to the suspension of the ground product and more particles were able to pass through the lower sieves. It is believed that the dispersing agent helped in destroying or reducing the surface tension of the suspension which might have partially blocked the apertures.

During the sieving of maize ground from samples of dry stage to 6 h of soaking, sieves of 7 and 14 mesh consisted of particles with endosperm. But as from 12 h of soaking and upwards, these first two sieves consisted of only flakes or testa of maize. This means that much of the endosperm has been ground because it became softened after long soaking. Therefore, it may be suggested that for effective wet grinding of maize, the grains should be soaked in water for at least 12 h before grinding. Whereas the sorghum and millet grains must be soaked at least for 2 h.

The effect of dispersing agent on sieving the suspension was actually determined by some control experiment when sieving was done without its addition. The prob-

Table 1. Effect of moisture content on grinding temperature.

SOAKING TIME (h)	MAIZE		SORGHUM		MILLET	
	AVERAGE M.C. (%, w.b.)	AVERAGE RISE IN TEMPERATURE (°C)	AVERAGE M.C. (%, w.b.)	AVERAGE RISE IN TEMPERATURE (°C)	AVERAGE M.C. (%, w.b.)	AVERAGE RISE IN TEMPERATURE (°C)
0 (Dry)	7.8	34.5	6.5	33	6.8	35
2	21.3	41.0	27.1	38	27.6	40
6	27.6	43.0	32.0	40	34.8	59
12	30.8	53.5	36.3	44	36.4	63
18	32.8	57.5	38.7	40	38.0	65
24	35.1	61.0	39.3	41	40.1	60
38	35.2	52.0	-	-	-	-
57	38.2	50.0	-	-	-	-
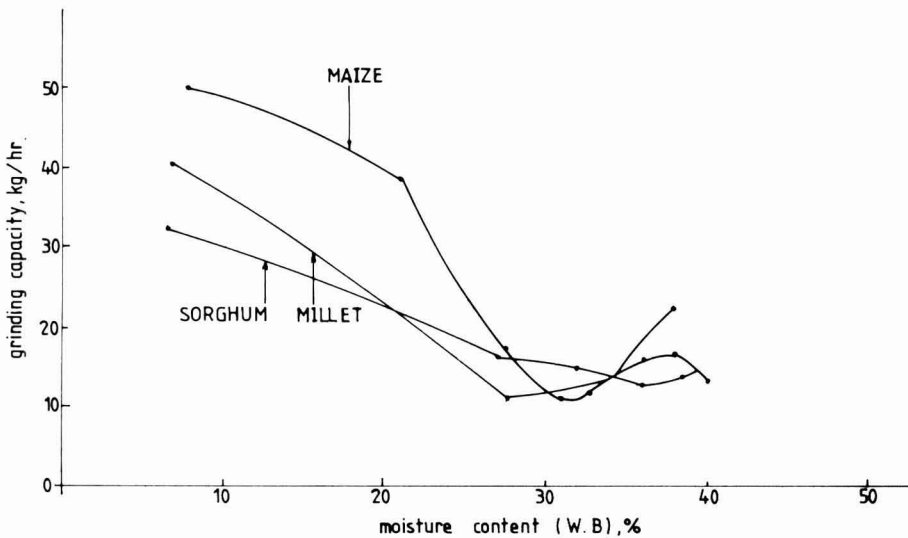
FIG. 1. EFFECT OF MOISTURE ON GRINDING CAPACITY.

lem sieves (less than 52 mesh) were observed to retain more fractions than when the dispersing agent was used.

Generally, it was observed that the unit weight of millet yields the largest amount of starch than sorghum and maize at constant grinding conditions.

Effect of Moisture Content on Distribution Parameters of Grains

Maize. Figure 2 is a log-probability plot of cumulative percent by weight against particle diameter from dry state (m.c. = 7.8%) to that soaked in water for 57 h (m.c. = 38.2%). In the dry grinding, the graph is a straight line indicating that the distribution was evenly spread throughout the sieves.

As from 2 h of soaking, the lower ends of the curves became concave indicating that the proportions of the lower sieve fractions were more than those of the upper fractions. In other words, the wet ground samples consisted of finer particles than that of dry grinding.

It is of interest to note that the distribution of 2 h and 6 h soaking (21.3 and 27.6% m.c.) consisted of coarse particles than when the maize was ground dry. Thus the two curves fall below that of dry grinding at the upper ends. This was physically observed to be true during grinding. This unusual behavior of ground maize soaked for few hours may still be linked with the Brekke's theory of increased tensile strength when dried cereal is suddenly exposed to moisture-rich environment.
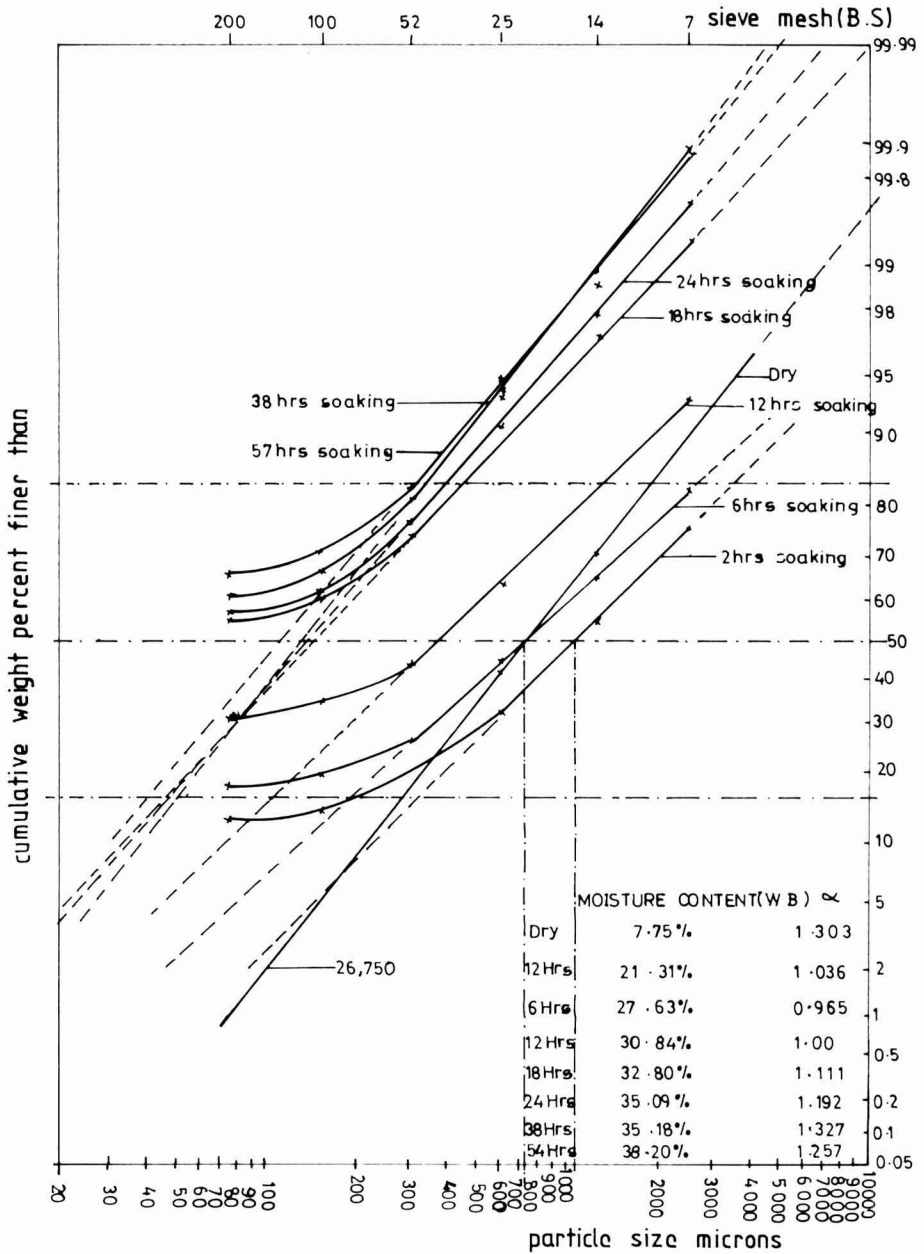
FIG. 2.   PARTICLE SIZE DISTRIBUTION OF MAIZE AS AFFECTED BY MOISTURE
CONTENT.

Table 2. Distribution parameters of ground maize at various moisture content.

SOAKING TIME (h)	MOISTURE CONTENT (%, w.b.)	GEOMETRIC MEAN DIAMETER d_{50} (microns)	DIAMETER AT 84% PROBABILITY, d_{84} (microns)	DIAMETER AT 16% PROBABILITY, d_{16} (microns)	GEOMETRIC STANDARD DEVIATION, s_{gw}	DISTRIBUTION MODULUS, α	SIZE MODULUS, k (microns)
0 (dry)	7.8	735.71	1928.57	283.50	2.63	1.3030	26750.00
2	21.3	1062.86	3535.71	321.92	3.33	1.0355	90000.00
6	27.6	721.43	2700.00	192.57	3.74	0.9654	95000.00
12	30.8	373.97	1373.56	105.78	3.67	1.0000	42000.00
18	32.8	151.72	465.82	48.35	3.07	1.1106	10000.00
24	35.1	137.50	392.86	48.35	2.86	1.1917	7200.00
38	35.2	135.00	344.44	52.17	2.55	1.3270	4600.00
57	38.2	115.00	333.33	40.91	2.90	1.2570	5000.00

Table 3. Distribution parameters of ground sorghum at various moisture content.

SOAKING TIME (h)	MOISTURE CONTENT (%, w.b.)	GEOMETRIC MEAN DIAMETER, d_{50} (microns)	DIAMETER AT 84% PROBABILITY, d_{84} (microns)	DIAMETER AT 16% PROBABILITY, d_{16} (microns)	GEOMETRIC STANDARD DEVIATION, sgw	DISTRIBUTION MODULUS, α	SIZE MODULUS, k (microns)
0 (dry)	6.5	582.61	1197.90	284.00	2.06	1.7860	8000.00
2	27.1	372.41	950.00	146.57	2.55	1.3270	13705.88
6	32.0	260.00	760.00	88.33	2.92	1.1504	16176.47
12	36.3	185.47	463.64	72.14	2.50	1.3470	8333.33
18	38.7	156.67	440.00	54.44	2.81	1.1917	6133.33
24	39.3	80.00	271.28	23.42	3.39	1.0355	8000.00

Table 4. Distribution parameters of ground millet at various moisture content.

SOAKING TIME (h)	MOISTURE CONTENT (%, w.b.)	GEOMETRIC MEAN DIAMETER, d_{50} (microns)	DIAMETER AT 84% PROBABILITY, d_{84} (microns)	DIAMETER AT 16% PROBABILITY, d_{16} (microns)	GEOMETRIC STANDARD DEVIATION, sgw	DISTRIBUTION MODULUS, α	SIZE MODULUS, k (microns)
0 (dry)	6.8	511.11	1065.00	245.00	2.080	1.698	8166.67
2	27.6	291.00	640.67	132.68	2.200	1.584	6000.00
6	34.8	126.47	282.50	57.08	2.230	1.585	2236.59
12	36.4	267.50	480.81	150.47	1.797	2.145	2236.59
18	8.0	285.00	500.00	162.86	1.754	2.169	2236.59
24	40.1	182.85	365.28	90.00	1.998	1.842	2236.59

Table 2 shows the determined constants. It could be argued that for good open circuit wet grinding of maize, the distribution modulus (α) should be about 1.32 which gives at least size modulus (k).

Sorghum. Figure 3 shows a log-probability plot of cumulative percent weight of sieve fractions of sorghum against particle diameter. It is observed that the curves of 2 h and 6 h soaking time fell below that of dry grinding. Their size moduli were larger than that of dry grinding. The size moduli of 18 h (m.c. = 38.7%) and 24 h (m.c. = 39.3%) were not better than that of dry grinding. It was also observed that the sample of 12 h soaking (m.c. = 36.3%) gave a very good size distribution representation, and its size modulus was the least.

Table 3 shows the distribution parameters of sorghum as affected by change in moisture content. It may be seen that the 12 h of soaking (m.c. = 36.3%) had the smallest size modulus and therefore may be recommended for grinding under wet conditions.

Millet. Figure 4 is a log-probability plot cumulative percent by weight against particle size for millet samples. The best distribution representation was found for the millet soaked for 6 h (m.c. = 34.8%). Table 4 gives the distribution parameters of millet as affected by change in moisture content. The geometric standard deviation which depicts the spread of the distribution is 2.23 for the best distributed sample.

Effect of Moisture Content On Geometric Diameter of Particles

A plot of the geometric mean diameter of ground particles $d50$, against moisture content is shown in Fig. 5. For maize, the curve rises from moisture content of 7.8% to about 25% after which it starts declining. This increase in geometric mean diameter immediately after soaking may be connected with the supposed increase in tensile strength of maize at the onset of soaking as discussed earlier.

The curve for sorghum continued to fall from the start to almost the end of the experiment. This indicated that the geometric mean diameter decreased with the increase in moisture content.

For millet the curve started rising at a moisture content of 34.5%. This shows that the geometric mean diameter of millet would continue to decrease with increase in moisture content till a critical point where further increase in moisture content would cause improper grinding resulting increased particle sizes. This critical moisture content coincides with the limit recommended for wet grinding of millet.

Effect of Moisture Content on Distribution Moduli

Figure 6 shows a plot of distribution moduli of maize, sorghum and millet against moisture content. It could be seen that the distribution modulus for maize falls from 1.3 at the initial moisture content of 7.8% to 1.00 at a moisture content of 23%. Hansen and Stewart (1965) stated that the distribution modulus of "1.00" shows complete
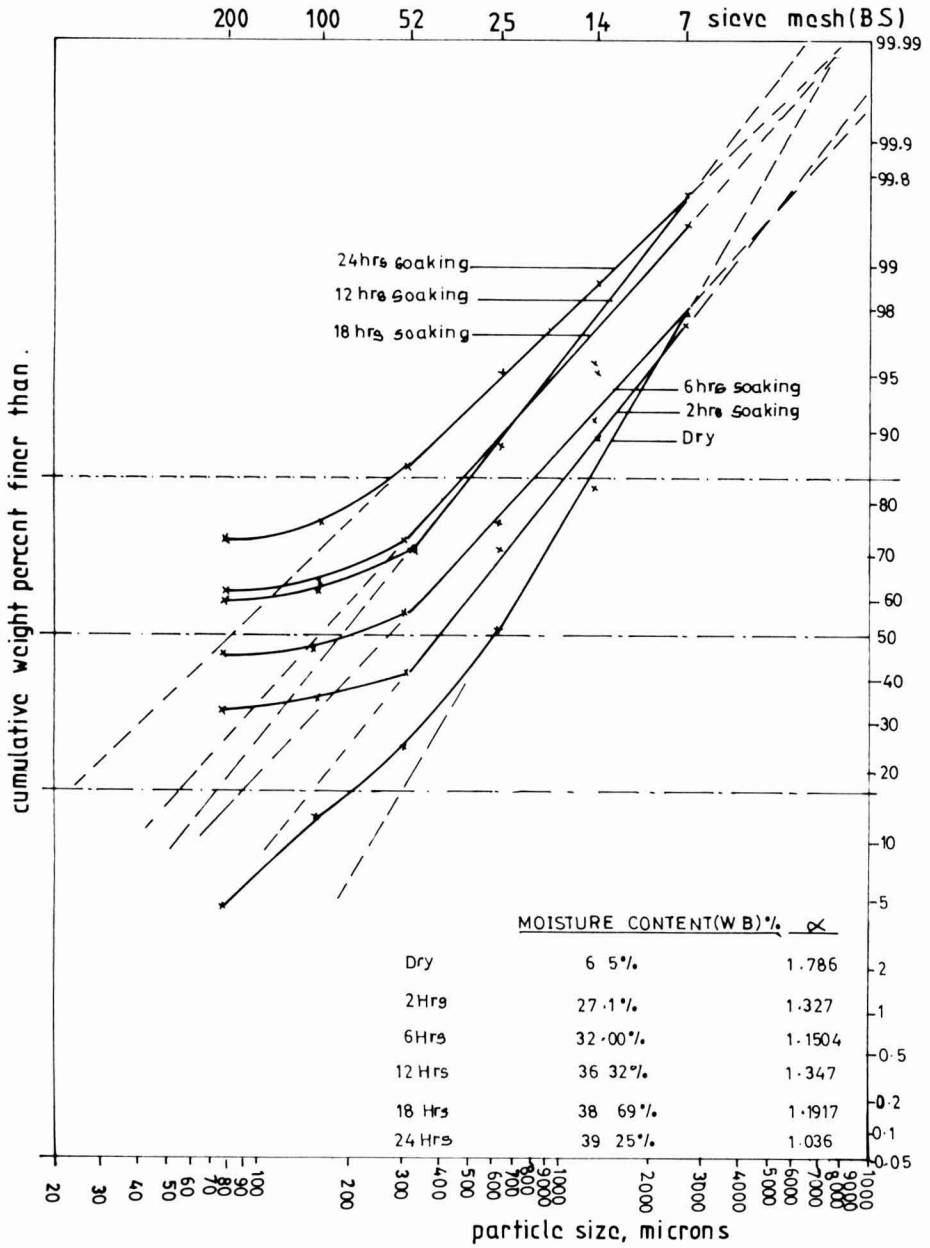
FIG. 3. PARTICLE SIZE DISTRIBUTION OF SORGHUM AS AFFECTED BY MOISTURE
CONTENT.
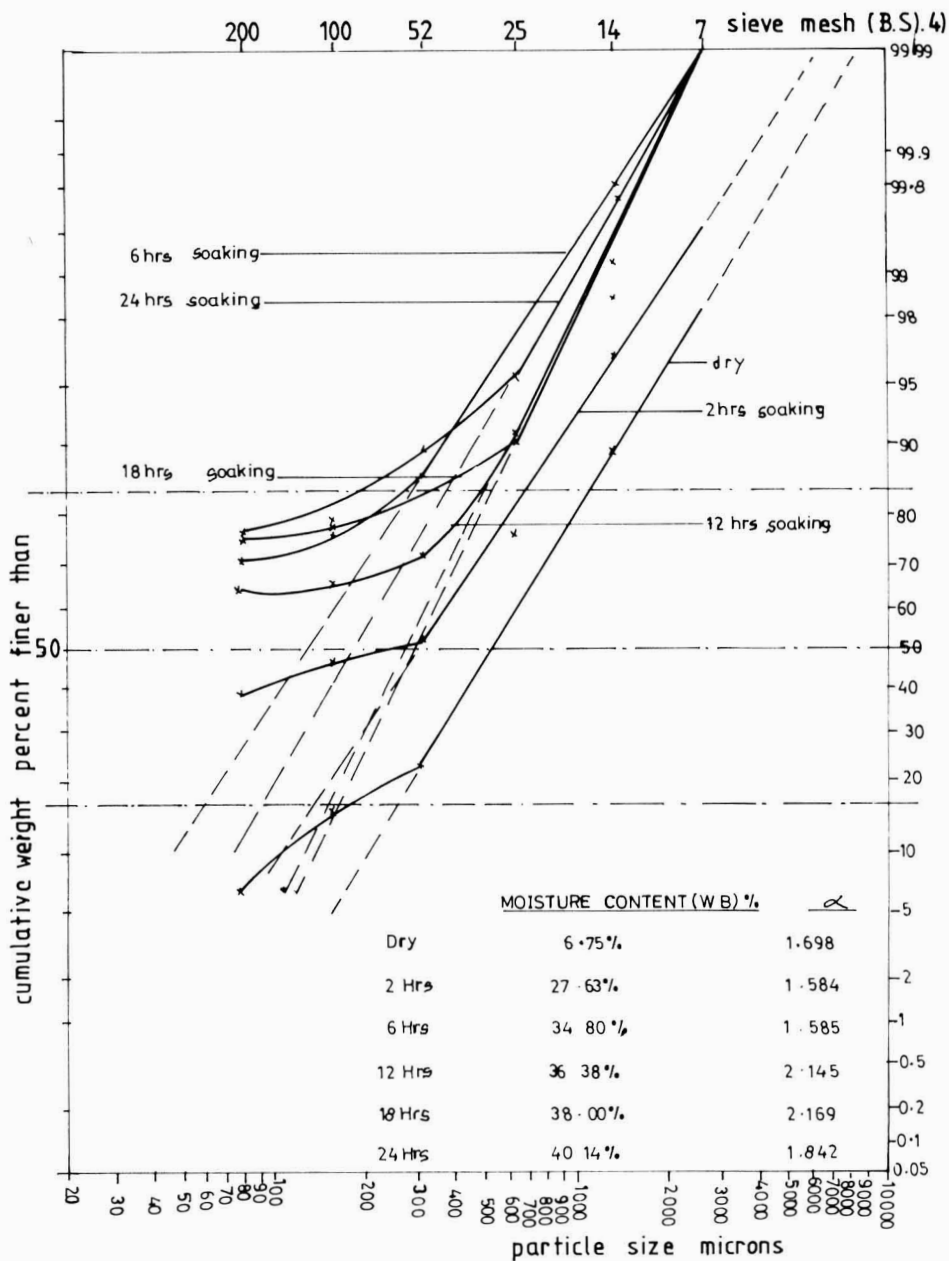
FIG. 4.   PARTICLE SIZE DISTRIBUTION OF MILLET AS AFFECTED BY MOISTURE
CONTENT.
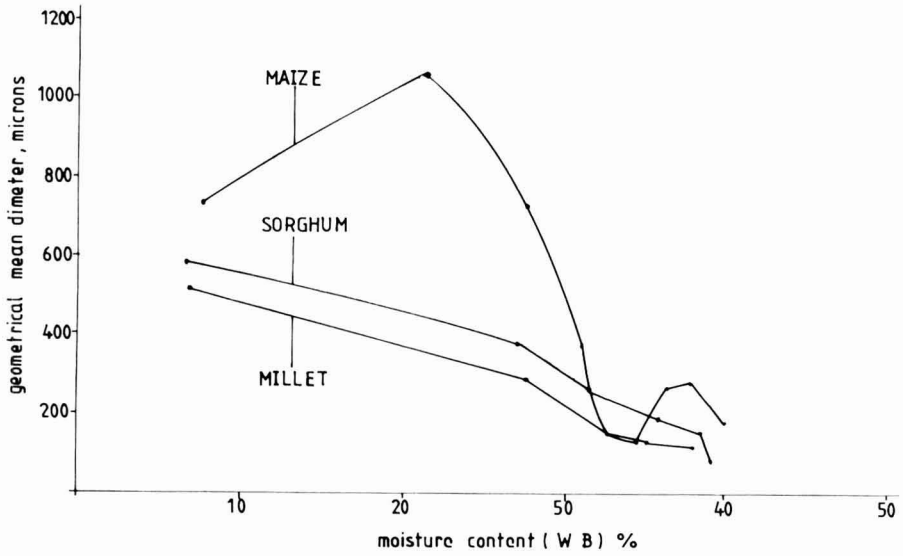
FIG. 5.   EFFECT OF MOISTURE CONTENT ON AVERAGE PARTICLE SIZE
DISTRIBUTION OF MAIZE, SORGHUM AND MILLET.
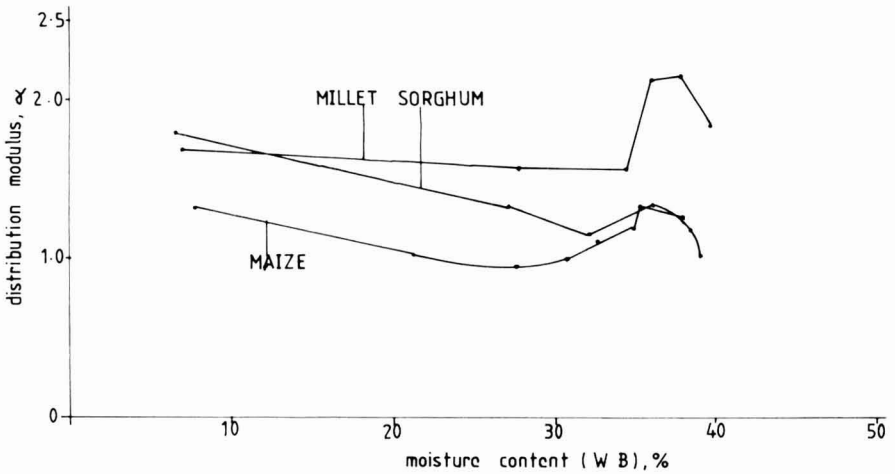
FIG. 6.   EFFECT OF MOISTURE CONTENT ON DISTRIBUTION MODULUS OF MAIZE,
SORGHUM AND MILLET.

brittleness of the material. The curve then falls below the 1.00 line and crosses it again at about a moisture content of 30.5% (another point of complete brittleness). This could indicate that maize might have undergone complete brittleness in two stages, the first perhaps with bigger fissures and the next with finer fissures. The first point at a 23% moisture content coincides with about 2 to 3 h of soaking and the last point of 30.5% moisture content coincides with about 12 h of soaking. In Fig. 2, the curves for 2 h and 12 h soaking time are seen to be partly below or too close to the curve of dry grinding, or rather their size moduli were bigger than that of dry grinding.

Sorghum and millet show a steady fall of the distribution modulus α, but does not reach the unity (1.00) line. This could mean that under the conditions of the experiment, sorghum and millet did not reach brittle stage.

Effect of Moisture Content on the Geometric Standard Deviation

Geometric standard deviation is a measure of the dispersion of the particles of the distribution relative to the mean value μ (the geometric mean diameter) which is at 50% probability. The greater the geometric standard deviation, the wider the probability of the distribution of the particles.

In this experiment, it may be suggested that the wider the dispersion, the more the nonuniform grinding and the greater the geometric standard deviation.

It can be seen from Table 2 that the geometric standard deviation for maize soaked 18 h was greater than those samples soaked beyond 18 h. In general, it could be said that the higher the moisture content of ground maize products the lower will be the geometric standard deviation.

In the case of sorghum, the minimum geometric standard deviation was when the grain was soaked for 12 h as shown in Table 3 (the moisture level recommended for optimum wet grinding).

With millet the geometric standard deviation was almost constant for 2 and 6 h of soaking, but beyond that, it decreased to another constant value for 12 and 18 h of soaking (Table 4); it could be said it decreased with increase in moisture content too. The curve for millet was almost constant from initial moisture content to about 34.5% (the point recommended for soaking in order to have good distribution of particles).

Effect of Dispersing Agent on Wet Sieving of Cereal Grains

A log-probability plot of cumulative percent weight against particle diameter for maize sieved with and without the dispersing agent is shown in Fig. 7. The tail end of the curves for distribution of sieving with dispersing agent is higher than one without. This shows that the dispersing agent breaks the surface tension caused by suspension and increases the ratio of lower sieve fractions.
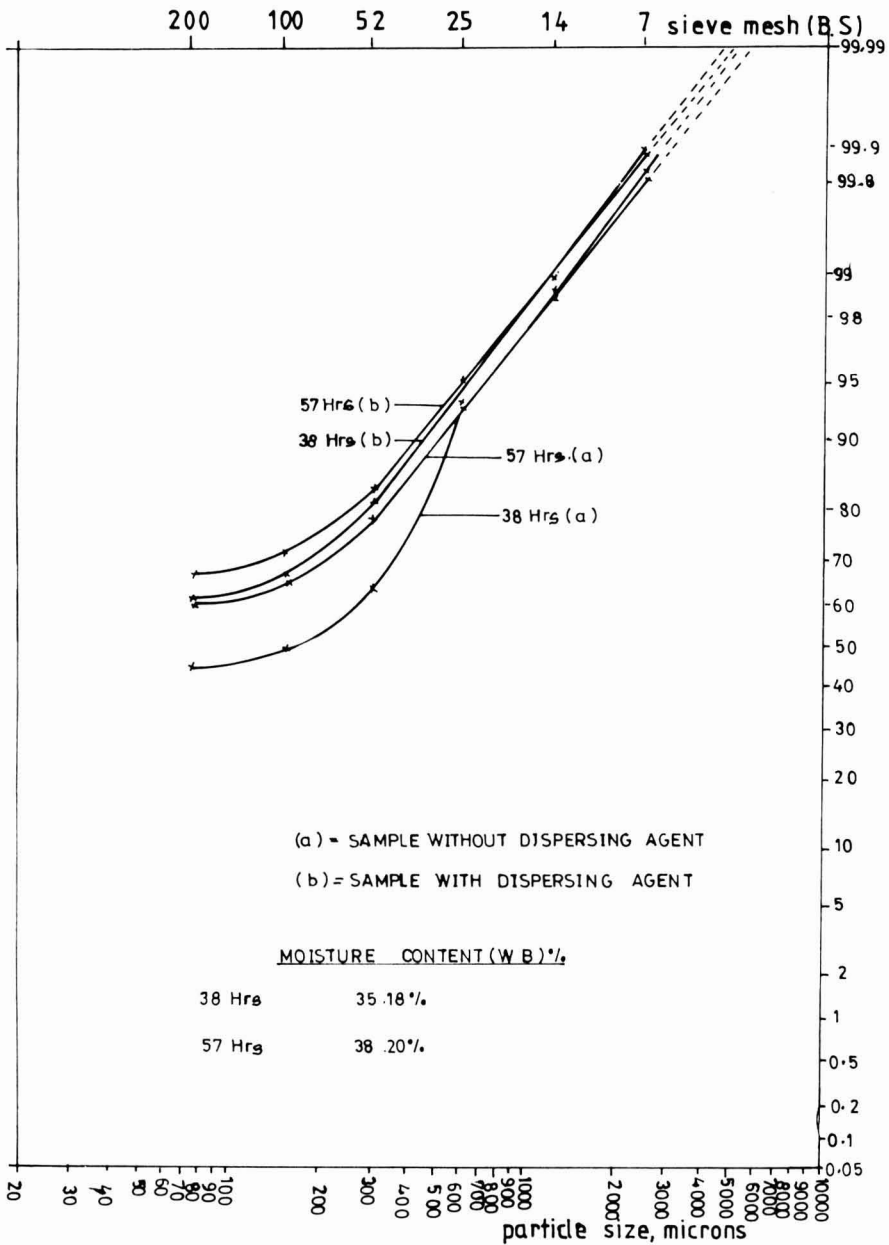
FIG. 7. EFFECT OF DISPERSING AGENT 'CALGON' ON PARTICLE SIZE DISTRIBUTION
OF MAIZE.

CONCLUSIONS

The following conclusions were drawn from this study:

(1) The geometric mean diameter of the particles of wet ground maize, sorghum and millet decrease with increase in moisture content except that the maize shows a deviation from this rule at the onset of soaking when the geometric mean diameter of the ground product becomes larger than in dry grinding.

(2) The average distribution moduli of maize and sorghum decrease with increase in moisture content. Millet showed an increase in distribution modulus with increase in moisture content.

(3) The geometric standard deviation for maize and millet decreased with increase in moisture content but that of sorghum was fairly constant.

(4) For good particle size distribution in wet grinding of these grains, maize should be soaked to a moisture content of at least 30.8%. Sorghum of low moisture content should be soaked to at most 36% moisture content. Millet should be soaked to about 34.8% moisture content.

(5) Dispersing agent was found to make sieving (especially in sieves of smaller apertures) effective. It destroyed or reduced surface tension which caused partial blockage to the sieve apertures during wet grinding.

REFERENCES

ASAE 1979/80 Year book. American Society of Agricultural Engineers, St. Joseph, MI.

BREKKE, O. L. 1968. Stress Crack formation in tempering of low-moisture corn and effect on degerminator performance. Northern Regional Research Laboratory, USDA, Peoria, IL.

CHUNG, C. J., CLARK, S. J., LINDHOLM, J. C., MC GINTY, R. J. and WATSON, C. A. 1977. Comminution parameters for wheat hardness measurement. Trans. ASAE. *20* (2), 375-379.

FUERSTENAU, D. W. and SULLIVAN, D. A. 1961. Size distribution and energy consumption in wet and dry grinding. AIME Transactions. Vol. *220*, 397-402.

HANSEN, R. C. and HENDERSON, S. M. 1972. Development of size distribution measurement and representation for ground cereal grains. Trans ASAE. *8* (2), 510-514.

HANSEN, R. C. and STEWART, R. E. 1965. Energy size reduction relations in agricultural grain comminution. Trans. ASAE. *8* (2), 230-234, 237.

HEADLEY, V. E. and PFOST, H. B. 1968. A comminution equation relating energy to surface area by the probability method. Trans. ASAE. *11* (3), 331-334, 338.

HENDERSON, S. M. and PERRY, R. L. 1976. *Agricultural Process Engineering,* 3rd Edition. AVI Publishing Co., Westport, CT.

JINDAL, V. K. 1975. Mechanics of hammer mill grinding of corn as related to its mechanical properties. Ph.D. Thesis. The Pennsylvania State University Park, PA.

PERRY, R. H. and CHILTON, C. H. 1973. *Chemical Engineering Handbook.* 5th Edition. McGraw Hill Book Co., New York.

RHIND, D. 1962. Breaking of rice in milling. Tropical Agric. *39*, 19.

*Correction for Table 1: Average rise in temperature is incorrect; average temperature is correct column title

JFS ABSTRACTS

Comparison of Stead Shear and Dynamic Viscoelastic Properties of Guar and Karaya Gums. (1984) P. I. Mills, J. L. Kokini. J. Food Sci. *49*, 1-4 + 9.

Steady shear and small amplitude dynamic viscoelastic properties of suspensions of guar gum and gum karaya in the range of shear rates/frequencies between 0.1 and 100 sec^{-1} were compared. For all concentrations of guar at small shear rates/frequencies steady viscosity (η) is equal to dynamic viscosity (η') when corresponding shear rates and frequencies are equal. At large shear rates, steady viscosity (η) is equal to complex viscosity (η^*), primary normal stress coefficient (ψ_1) is approximately equal to ($2\eta''/\omega$). For gum karaya it was shown that (η''/ω) is nonlinearly related to primary normal stress coefficient (ψ_1) and dynamic viscosity (η'') is nonlinearly related to steady viscosity (η').

Thermal Properties of Bentonite-water Disperstions Used for Modeling Foods. (1984) A. Niekamp, K. Unklesbay, M. Ellersieck. J. Food Sci. *49*, 28-31.

Selected thermal properties (moisture content, density, heat capacity, thermal conductivity) were measured for ten bentonite-water dispersions used in food modeling and for betonite powder. As the bentonite concentration increased, significant ($P < 0.05$) increases in thermal conductivity and density, and significant ($P < 0.05$) decreases in heat capacity were revealed. Measured heat capacity values were lower than calculated values of heat capacity which were derived from three formulas recommended for foods.

A Physiochemical Model for Extrusion of Corn Starch. (1984) M. H. Gomez, J. M. Aguilera. J. Food Sci. *49*, 40-43 + 63.

Corn starch extruded at 32.9, 29.2, 24.5, 22.5, 15.9 and 14.2% moisture was analyzed for expansion ratio, enzyme susceptibility, water solubility index, water absorption index, degree of gelatinization, paste viscosity and heat of gelatinization. A model system based on the combination of raw, gelatinized and dextrinized starch was used to represent the physicochemical properties of the extrudates. Reducing extrusion moisture content resulted in a progressive change from gelatinized-like to dextrinized-like properties. Maximum gelatinization was observed at about 28-29% moisture. Below 20% moisture, dextrinization becomes predominant during highshear cooking-extrusion. Scanning electron micrographs also validate the assumptions of the model.

Identification of Key Textural Attributes of Fluid and Semi-solid Foods Using Regression Analysis. (1984) J. L. Kokini, M. Poole, P. Mason, S. Miller, E. F. Stier. J. Food Sci. *49*, 47-51.

Regression analysis was used to identify key attributes from 15 textural terms generated by a panel for 27 fluid and semi-solid commercial foods. A search using single in-

dependent variables showed that "thick" gave the best average R² with a value of 0.548; a search with two independent variables showed that "thick" and "soft" gave the best average R² of 0.748; a search with three attributes showed that "slippery." "thick," and "soft" gave the highest R² values of 0.803. The final equations provided a set of regression parameters which can be used to predict twelve textural attributes from scores obtained for "thick," "soft," and "slippery."

Flow Profiles of Aqueous Dispersed Pectins.(1984) R. H. Walter, R. M. Sherman. J. Food Sci. *49*, 67-69.

The viscosity numbers of dilute, aqueous, pectin dispersions in 0.04 molal tartaric acid were measured as a function of pectin concentration. The flow characteristics were concluded to be pectin-specific rather than class-specific. The equation describing the linear relationship involves a squared expression of the factors that influence the mass and size of the macromolecules. As a result, small differences in methoxyl content, polydispersity, location of carboxyl groups, etc. were exaggerated to give each pectin nearly unique orientation in a coordinate plane, defined by an apparent-viscosity factor and the reciprocal, absolute temperature.

Chitosan Membranes for Reverse Osmosis Application. (1984) T. Yang, R. R. Zall. J. Food Sci. *49*, 91-93.

Alkab resistant reverse osmosis membranes were fabricated by spreading solutions of chitosan, a poly-N-acetyl glucosamine, in 2.0% acetic acid on a glass plate. The membrane had a flux rate of 1.67×10^{-3} cm³/cm²/sec and a salt rejection capability of 78.8% with 0.2% NaCl at 680 psi. Addition of 40% polyethylene glycol to the membrane casting solution increased permeability, while 10% chloromethyl oxirane improved durability of the membranes.

Flow Behavior of Liquid Whole Egg During Thermal Treatments (1984) M. Hamid-Samimi, K. R. Swartzel, H. R. Ball, Jr. J. Food Sci. *49*, 132-136.

Costs of handling and loss of functional properties of frozen liquid whole egg (LWE) has stimulated interest in a refrigerated product. To maintain adequate shelf life at refrigeration temperatures a heat treatment more severe than normal pasteurization may be needed. To establish limits for the thermal treatment and to prevent possible damage to the pasteurization system due to coagulation of the product, flow properties of LWE during pasteurization were investigated. Utilizing a cone and plate viscometer, egg viscosity was determined at shear rates between 115 and 450 sec. Test temperatures varied from 20-75 °C and heat treatment durations ranged from 0.5-10 min. Percent protein denaturation for each treatment was also determined and correlated to the flow properties Above 60 °C viscosities were shear rate dependent while below this temperature flow properties were approximately Newtonian

Mathematical expressions were developed for viscosity as a function of time, temperature and shear rate.

Modeling the Thermal Conductivity of Cooked Meat. (1984) M. G. R. Perez, Covelo. J. Food Sci. *49*, 152-156.

The thermal conductivity of cooked meat under different thermal treatments is measured and a mathematical model for its prediction is developed. Apparent and real densities, thermal conductivity and water content were evaluated on the cooked samples. The thermal conductivity showed good correlation with the water content. Values were found to be independent of the thermal history during cooking. Experimental results showed a good agreement with the proposed mathematical model that considers meat as composed by air and water spheres distributed over a matrix of dry fiber. Values for the parameters involved are provided, as well as expressions for the shrinkage of samples taking into account the incorporation of air during cooking.

Supercritical Fluid Extraction of Dry-milled Corn Germ with Carbon Dioxide. (1984) D. D. Christianson, J. P. Friedrich, G. R. List, K. Warner, E. B. Bagley, A. C. Stringfellow, G. E. Inglett. J. Food Sci. *49*, 229-232 + 272.

Dry milled corn germ was extracted with supercritical carbon dioxide ($SC-CO_2$) at 5,000-8,000 psi and 50 °C. CO_2-extracted out was lower in free fatty acids and refining loss, and was lighter in color when compared with a commercial explicit milled crude oil. Total unsaponifiable and docopherol contents were similar for both oil types. The defatted highly friable flour has a shelf-stable moisture content of 2-3% and good flavor quality. The flour contains 20% protein with good animal acid balance, meeting FAO specifications for food protein supplements. High pressure $SC-CO_2$ extraction also denatures the proteins including oxidative enzymes. Peroxidase activity in reduced tenfold in $SC-CO_2$-extracted flour when compared with hexane-extracted flours. Storage tests for 5 wk at 38 °C and for 2 months at 25 °C show that flavor quality of untoasted $SC-CO_2$ defatted germ flour is maintained even under these extreme conditions.

AUTHOR INDEX

SUBJECT INDEX

GUIDE FOR AUTHORS

Typewritten manuscripts in triplicate should be submitted to the editorial office. The typing should be double-spaced throughout with one-inch margins on all sides.

Page one should contain: the title, which should be concise and informative; the complete name(s) of the author(s); affiliation of the author(s); a running title of 40 characters or less; and the name and mail address to whom correspondence should be sent.

Page two should contain an abstract of not more than 150 words. This abstract should be intelligible by itself.

The main text should begin on page three and will ordinarily have the following arrangement:

Introduction: This should be brief and state the reason for the work in relation to the field. It should indicate what new contribution is made by the work described.

Materials and Methods: Enough information should be provided to allow other investigators to repeat the work. Avoid repeating the details of procedures which have already been published elsewhere.

Results: The results should be presented as concisely as possible. Do not use tables *and* figures for presentation of the same data.

Discussion: The discussion section should be used for the interpretation of results. The results should not be repeated.

In some cases it might be desirable to combine results and discussion sections.

References: References should be given in the text by the surname of the authors and the year. *Et al.* should be used in the text when there are more than two authors. All authors should be given in the Reference section. In the Reference section the references should be listed alphabetically. See below for style to be used.

DEWALD, B., DULANEY, J. T. and TOUSTER, O. 1974. Solubilization and polyacrylamide gel electrophoresis of membrane enzymes with detergents. In *Methods in Enzymology,* Vol. xxxii, (S. Fleischer and L. Packer, eds.) pp. 82–91, Academic Press, New York.

HASSON, E. P. and LATIES, G. G. 1976. Separation and characterization of potato lipid acylhydrolases. Plant Physiol. *57*, 142–147.

ZABORSKY, O. 1973. *Immobilized Enzymes,* pp. 28–46, CRC Press, Cleveland, Ohio.

Journal abbreviations should follow those used in *Chemical Abstracts.* Responsibility for the accuracy of citations rests entirely with the author(s). References to papers in press should indicate the name of the journal and should only be used for papers that have been accepted for publication. Submitted papers should be referred to by such terms as ''unpublished observations'' or ''private communication.'' However, these last should be used only when absolutely necessary.

Tables should be numbered consecutively with Arabic numerals. The title of the table should appear as below:

Table 1. Activity of potato acyl-hydrolases on neutral lipids, galactolipids, and phospholipids

Description of experimental work or explanation of symbols should go below the table proper. Type tables neatly and correctly as tables are considered art and are not typeset. Single-space tables.

Figures should be listed in order in the text using Arabic numbers. Figure legends should be typed on a separate page. Figures and tables should be intelligible without reference to the text. Authors should indicate where the tables and figures should be placed in the text. Photographs must be supplied as glossy black and white prints. Line diagrams should be drawn with black waterproof ink on white paper or board. The lettering should be of such a size that it is easily legible after reduction. Each diagram and photograph should be clearly labeled on the reverse side with the name(s) of author(s), and title of paper. When not obvious, each photograph and diagram should be labeled on the back to show the top of the photograph or diagram.

Acknowledgments: Acknowledgments should be listed on a separate page.

Short notes will be published where the information is deemed sufficiently important to warrant rapid publication. The format for short papers may be similar to that for regular papers but more concisely written. Short notes may be of a less general nature and written principally for specialists in the particular area with which the manuscript is dealing. Manuscripts which do not meet the requirement of importance and necessity for rapid publication will, after notification of the author(s), be treated as regular papers. Regular papers may be very short.

Standard nomenclature as used in the engineering literature should be followed. Avoid laboratory jargon. If abbreviations or trade n   s are used, define the material or compound the first time that it is mentioned.

EDITORIAL OFFICE: Dr. D. R. Heldman, Edi or, Journal of Food Process Engineering, Campbell Institute for Research and Technology, Campbell Place, Camden, New Jersey 08101 USA.

CONTENTS

-๑ ก.ค 2528